ACS ENVIRONMENTAL Au
AN OPEN ACCESS JOURNAL OF THE AMERICAN CHEMICAL SOCIETY

pubs.acs.org/environau
Review

Recent Advances in Technologies for Phosphate Removal and Recovery: A Review

Mallikarjuna N. Nadagouda,* Gaiven Varshney, Vikas Varshney, and Charifa A. Hejase

Cite This: ACS Environ. Au 2024, 4, 271−291
Read Online

ACCESS | Metrics & More | Article Recommendations

ABSTRACT: Phosphorus is a nonrenewable resource, yet an essential nutrient in crop fertilizers that helps meet growing agricultural and food demands. As a limiting nutrient for primary producers, an excess amount of phosphorus entering water sources through agricultural runoff can lead to eutrophication events downstream. Therefore, to address global issues associated with the depletion of phosphate rock reserves and minimize the eutrophication of water bodies, numerous studies have investigated the removal and recovery of phosphates in usable forms using various chemical, physical, and biological methods. This review provides a comprehensive and critical evaluation of the literature, focusing on the widely employed adsorption and chemical precipitation for phosphate recovery from various wastewaters. Several experimental performance parameters including temperature, pH, coexisting ions (e.g., NO_3^-, HCO_3^-, Cl^-, SO_4^{2-}), surface area, porosity, and calcination are highlighted for their importance in optimizing adsorption capacity and struvite crystallization/precipitation. Furthermore, the morphological and structural characterization of various selected adsorbents and precipitated struvite crystals is discussed.

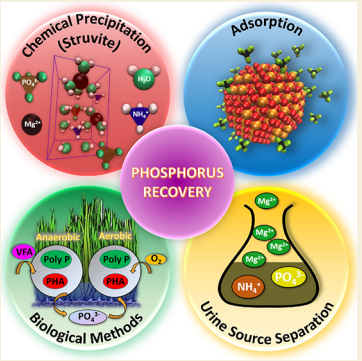

KEYWORDS: *eutrophication, nutrient recovery, phosphate, adsorption, chemical precipitation, struvite, fertilizers, bioavailability, wastewater treatment*

1. INTRODUCTION

Phosphorus is a crucial mineral nutrient for all living forms. It is used in industry and agriculture as a fertilizer and for controlling bio-organism growth. In aquatic environments, phosphorus is typically found in the form of phosphates, which can be either organic (i.e., bound to plant or animal tissue) or inorganic (i.e., orthophosphates, polyphosphates, etc.). Among these different forms, orthophosphates are the only form of phosphorus that can be utilized by plants, bacteria, and algae and are formed by hydrolysis or microbial mobilization of other pentavalent forms.[1] As phosphates cycle through the aquatic ecosystem, they change form from inorganic to organic. For example, dissolved inorganic phosphate is consumed by aquatic plants and converted to organic phosphate as it binds to their tissues. Organic phosphates are then consumed by marine animals that eat aquatic plants. When aquatic organisms die or excrete waste, their organic phosphates sink to the bottom of the water column, where decomposition by bacterial species converts them back to either dissolved or particulate-bound inorganic phosphates. Apart from their importance in the aquatic environment, phosphates are also utilized in many diverse areas such as photocatalysis,[2] electrochemistry,[3] and bioceramics,[4] and as inhibitors to prevent calcium scale buildup and lead corrosion in drinking water distribution systems.[5]

1.1. Nutrient Pollution and Its Environmental Impact

Although phosphorus is essential for preserving aquatic ecosystems, its increased concentration in aquatic environments has both environmental and economic impacts. For example, high phosphorus concentrations (over 0.1 mg/L) are often associated with several million tons of phosphorus-containing wastewater directly discharged into water bodies such as lakes, rivers, etc. This process occurs through the decomposition of organic materials, disposal of industrial wastewater, discharge of urban sewage, runoff of animal manure and animal feed, weathering of rocks, and side effects of using fertilizers in agriculture.[6−10] These high concentrations result in accelerated algae growth and other consequent problems.[11] This phenomenon is often termed nutrient pollution, which also includes nitrogen and potassium waste, and is considered one of the most costly, extensive, and severe environmental problems.[12,13]

To limit the phosphorus content in aquatic environments, the World Health Organization (WHO) has set a guideline for a maximum discharge limit of phosphorus at 0.5−1 mg/L.[14]

Received: November 7, 2023
Revised: May 21, 2024
Accepted: May 21, 2024
Published: September 11, 2024

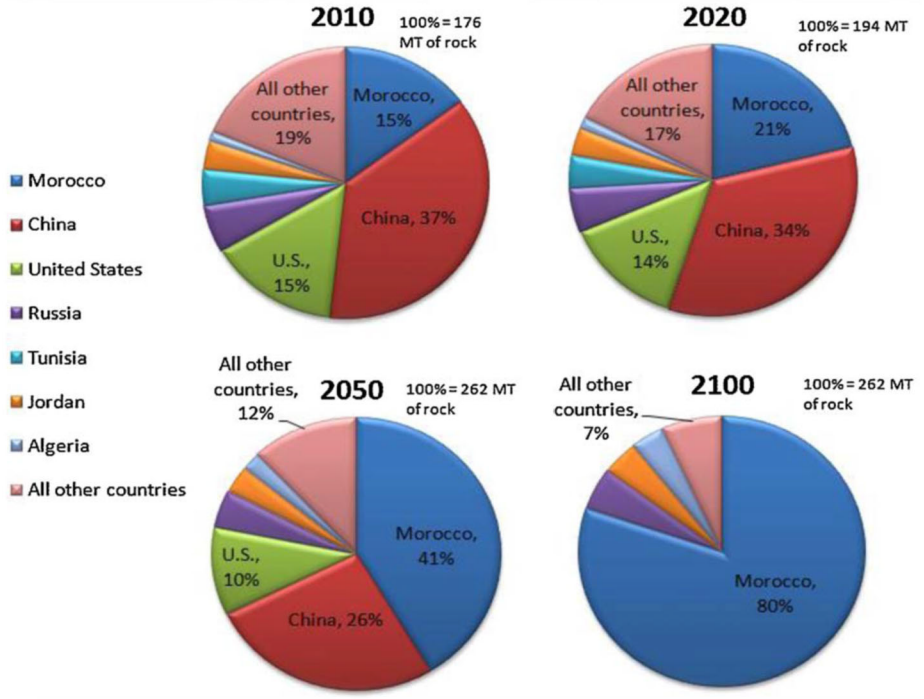

Figure 1. Estimated future worldwide share of phosphate rock production. Adapted with permission from Cooper et al.[17] (Copyright 2011 Elsevier).

Similarly, to control algae growth, phosphate concentrations should not exceed: (i) 0.05 mg/L in streams that discharge into lakes or reservoirs, (ii) 0.025 mg/L within lakes or reservoirs, and (iii) 0.1 mg/L in streams, rivers, or flowing waters that do not discharge into lakes or reservoirs.[15] However, problematic nutrient levels (concentration thresholds over which it can be termed nutrient pollution) vary from one region to another due differences in climate, geology, and soil type.

1.2. Phosphorus Extraction as Wastewater Recovery: A Win-Win Situation

The demand for phosphate is constantly increasing for industrial and agricultural purposes.[16] Commercially, phosphate is acquired from mining the "phosphate rock," or rocks largely consisting of calcium phosphate (apatite), most of which is used for fertilizer production.[17] In the past half-century, phosphorus rock has been the preferred phosphate fertilizer material for food production and crop growth, and its demand has increased drastically since the mid-19th century. This sudden and drastic increase is associated with the rapid population growth in the late 20th century when the global food demands could not be fulfilled without the use of phosphate-based fertilizers.[18]

The global phosphate mining is approximately five times more than the amount of phosphate used for food production purposes.[19] Cordell et al. used substance flow analysis (SFA) to quantify phosphate flows throughout agricultural, human food, and sewage systems. With SFA, phosphorus can be traced through the entire food production and consumption system (from mining to eventual consumption), and the loss of phosphate throughout the system can be quantified. The different stages include mining, producing fertilizer, applying fertilizers to agricultural soils, harvesting crops, processing, consuming, and excreting food while flowing from the system at various junctures to either the natural environment or recirculating back to the food system. This analysis showed that significant losses occur throughout the system (i.e., from mining to food consumption). To minimize such losses, a unified approach must be pursued: (i) minimize phosphorus losses during the cropping and harvesting phases, (ii) mitigate the losses in the food chain, (iii) incorporate alternative renewable phosphorus resources (e.g., manure, human excreta, food residues), and (iv) reduce the overall phosphorus demand (e.g., optimize soil carbon for improving phosphate availability).[19]

As a nonrenewable resource, phosphate rock reserves are limited in quantity, and thus, economically viable phosphate based on rock extraction is being depleted rapidly. Even though there is no consensus about the remaining time that phosphate reserves will be sustainable (estimates range from 60 years to several hundred years), it is widely acknowledged that extractable phosphate will eventually be fully depleted.[20] Countries such as the United States, China, and Morocco control the majority of global phosphate rock reserves (Figure 1). Among these countries, Morocco has considerably larger reserves than any other, as countries with large reserves (e.g., the United States and China) have partially exhaustsed theirs over the past century. According to Figure 1. Cooper et al.'s analysis shows that in the coming decades, Morocco will be responsible for over 20%, 40%, and 80% of the global phosphorus production by 2020, 2050, and 2100, respectively.[17]

In addition to phosphate depletion, phosphate rock mining has several negative environmental impacts, including the deterioration of land, air, and water quality.[21] It is speculated that recycling and reuse of phosphates released into the environment may alleviate the economic and environmental problems associated with phosphate rock mining. Furthermore, as there are no known alternatives for phosphates in food production and since elemental phosphorus cannot be synthesized in a laboratory, phosphate recovery from pollutants is imperative to meet current and future demands.[19] To meet future phosphorus demand, several efforts have already been made in a few countries to recover phosphorus from wastewater as struvite (a well-known phosphate-based fertilizer) and

https://doi.org/10.1021/acsenvironau.3c00069
ACS Environ. Au 2024, 4, 271−291

Table 1. Merits and Demerits of Various Methods Used for Phosphorus Removal and Recovery

S. No.	Methods	Merits	Demerits	Ref
1	Chemical precipitation	• Easy to design • Simple to start up and operate • Reliable, flexible, and easily operated	• Slow reaction by producing additional amount of sludge • Costly and time-consuming disposal and neutralization of the effluent • Inadequate efficiency for dilute phosphorus solutions • Suitable at high concentrations • Difficult to separate chemically bonded phosphate (P) (e.g., Fe/Al precipitates), making efficient P recovery unlikely for further use • Alkali or acid neutralization of effluent is required	30−32
2	Adsorption	• Minimal sludge production • Less disposal problems • Fast, highly efficient, and inexpensive • Possible recovery depending on phosphate sorption mechanism and type of adsorbent (i.e., cost and performance) • Phosphate removal at low concentrations • Availability of different adsorbents • Adsorbent reuse	• Competitive foreign ion adsorption	33,34
3	Membrane filtration	• Excellent removal • No waste production • Ion and size selective • Performance depends heavily on the pH of operation • Some membranes are pH sensitive • Membrane concentrates can be used for phosphate recovery	• Expensive and inefficient • Require extensive pretreatment for suspended solids reduction to prevent membrane fouling • Generate a reject waste stream • Low selectivity in the presence of competing anions	35
4	Ion Exchange	• Effective even at low phosphate concentration • No waste production	• Require high regeneration cost • Issue of sludge disposal due to precipitation or coagulation processes • High amount of resins required • Chemicals require for regeneration • Limited resin life • P recovery through post-treatment	36
5	Constructed wetlands	• Environmentally sensitive • Low energy consumption • Low cost • Same location establishment as that of wastewater	• Area-intensive • Complicated and difficult to sustain process • Unrealistic P recovery from the substrate volume of constructed wetlands	37
6	Crystallization	• Recyclable, slow-release rate • Low or no heavy metals • Less evaporation loss of nitrogen • Struvite could be directly used as a soil fertilizer	• Sometimes heavy metal coprecipitated •Relatively high cost for struvite production • Long reaction time • Limited to high value crops	38, 39
7	Enhanced biological phosphorus removal (EBPR)	• No chemicals required • Cost effective • Highly efficient	• Low effectiveness at low phosphate concentrations • Infrastructural cost required • Sludge production • Carbon and nitrogen source required • Trade-off between P recovery and sludge treatment cost	1

hydroxyapatite and subsequently use it for fertilization.[22,23] If struvite could be recovered from wastewater treatment plants worldwide, phosphate rock mining could be reduced by 1.6% annually, corresponding to an annual recovery of 0.63 million tons of phosphorus.[24] Recovering struvite from wastewaters could also alleviate rising fertilizer prices in the future, produce a new revenue stream, and subsequently reduce the demand for mining phosphate rocks.

Various methods and techniques have been developed to remove and recover phosphorus from wastewater. These methods include chemical methods (adsorption, chemical precipitation, struvite crystallization), biological methods (enhanced biological phosphate removal (EBPR), algae, plants), physical methods (nano- and microfiltration, reverse osmosis, ion exchange), and urine source-separation.[25−29] Table 1 lists the merits and demerits of each method for comparative purposes. As seen from the table, the adsorption process is

https://doi.org/10.1021/acsenvironau.3c00069
ACS Environ. Au 2024, 4, 271−291

Table 2. Selected Adsorbents Employed for the Removal of Phosphate from Wastewater

Adsorbent	Method	Initial phosphate conc. (mg/L)	Temperature	pH	Adsorption capacity (mg/g)	Best equilibrium model to fit data	Desorption solution and efficiency (%)	Ref
Peat	Batch	23	25	6.5	8.91	Langmuir	0.01 M KCl; 39.2%	53
Crawfish biochar	Batch	1−50	25	6	70.9	Freundlich and Langmuir	N/A	54
Mg−Al hydrotalcite loaded kaolin clay	Batch	25	25	2.5−9.5	11.92	Langmuir	N/A	7
Magnesium carbonate with cellulose pellets	Batch	330 mg/L	22.7	7	96.4	Langmuir	0.1 M HCl and 0.1 M NaOH; 4.4%	55
Active red mud	Batch	155	25	7	202, 155	Langmuir	N/A	56
Fe/$CaCl_2$	Batch	200	25	7	17	Langmuir	N/A	57
Fe/$MgCl_2$					17			
Fe/$MgCO_3$					16.9			
Fe/$CaCO_3$					16.9			
Zinc oxide betaine modified biochar nanocomposite	Batch	10−500	25	2−10	27.34, 75.01, 77.91	Langmuir	N/A	58
Ce hydroxide nanoparticles encapsulated inside an animated microporous polystyrene host D201	Batch, Column	1.83	25	7	36.4	-	10% NaOH and 5% NaCl; 95%	59
Nanoscale zerovalent iron confined in anion exchange resin	Batch, Column	5−750	25	7.2	56.27	Langmuir	5% NaCl and 5% NaOH; 95.9%	60
Zr-modified clays (kaolinite, montmorillonite, vermiculite	Batch	10	20	7	Zr-KT: 9 Zr-MT: 15 Zr-VT: 9.5	Langmuir, Freundlich	N/A	61
Ce/Fe bimetallic metal organic framework (MOF)(Ce/FcDA/FA-MOFs)	Batch	50−300	25	3−11	530.25	Freundlich	N/A	62
La-modified tourmaline	Batch	5	25	7	108.7	Langmuir	N/A	63
La hydroxide	Batch	100	24	2.5−12	107.53	Langmuir	3 and 12 M NaOH	45
Lanthanum-doped aminated graphene oxide/ aminated chitosan microspheres (La-AmGO@AmCs)	Batch	20−100	25−40	6.8	125	Langmuir	0.1 M NaOH	64
Fe−Mg−La trimetal composite	Batch	20	N/A	6	415.2	Langmuir	0.5 M NaOH	15
Fe−Zr binary oxide	Batch	5−10	25	8.5, 5.5	24.90, 33.40	Langmuir	0.5 M NaOH (53%)	65
Nanostructured Fe−Cu binary oxide	Batch	5	25	7	35.2	Langmuir	0.5 M NaOH; 69%	6
Fe−Mn binary oxide	Batch	5, 10	25	5.6	36	Freundlich	0.1 M NaOH; 90%	66
Nano Ce−Zr binary oxide	Batch	5, 10	25	6.2	112.23	Langmuir	0.001−0.5 M NaOH; 65−97%	67
Nanostructured Fe−Ti binary oxide	Batch	2.5, 5	20	6.8	35.4	Langmuir	0.1 M NaOH	68
E33	Batch, column	80	21	6−9	26.8	Langmuir	N/A	69
E33/AgI					19.3			
E33/AgII					28.0			
E33/Mn					17.8			

considered an effective route due to its low cost, ease of operation, easy application for phosphate removal in small-scale treatment facilities, and suitability for wastewater with low phosphate concentrations.

Given the immense volume of published literature on removing phosphate from wastewater and human waste, it is difficult to comprehensively cover all aspects of phosphate recovery in a single review. In this review, three important aspects of phosphorus removal are highlighted. First, adsorption methods for phosphate removal and recovery, including the morphological characterization of the adsorbents, adsorption mechanisms of phosphates on the adsorbents, assessment of adsorption capacity, and the effect of various parameters, will be discussed. The next topic will be the extraction of struvite (struvite crystallization) using chemical precipitation. In phosphate recovery for fertilization, struvite plays an integral role as it is an great important slow-release fertilizer. The third aspect focuses on the struvite formation mechanism, the effect of different experimental parameters on the efficiency of struvite crystallization, morphology characterization, competition with other phosphate crystal forms, and its fertilization aspects.

2. ADSORPTION METHOD FOR PHOSPHORUS RECOVERY AND EXTRACTION

To alleviate environmental and economic concerns for phosphorus recovery, considerable attention has been focused toward the adsorption method. Adsorption is a mass transfer process that involves one or more solute particles (atoms, ions, or molecules) present in the liquid or gas phase to adhere and/or accumulate on the surface of a solid adsorbent. These particles are held together either by physical intermolecular interactions

https://doi.org/10.1021/acsenvironau.3c00069
ACS Environ. Au 2024, 4, 271−291

(i.e., electrostatic and dispersive interactions) or by chemical interactions (i.e., chemical bonds). Compared to other techniques, adsorption is one of the most promising and practical techniques for phosphate recovery in water treatment due to its advantages of high removal efficiency without producing harmful byproducts, cost-effectiveness, and design flexibility.[40−45] In addition, adsorption also possesses the benefits of (i) being applicable at low concentrations,[46] (ii) producing little sludge, (iii) having potential as both batch and column processes, and (iv) having potential for recyclability (regeneration and reusability) of adsorbents, all of which can further reduce the waste and cost.[47−50]

Unlike absorption, adsorption is a surface process that occurs at the surface boundary, where the adsorbed particles do not diffuse into the bulk phase. The substances adsorbed on the surface are referred to as adsorbates, while the solid phase material that adsorbs the substances onto its surface is called the adsorbent.[16] As a surface phenomenon, factors affecting adsorption include the adsorbent's specific surface area, particle size, contact/residence time, adsorbate's solubility and affinity toward the adsorbent (i.e., electrostatic and/or dispersive interactions), and solution conditions (e.g., pH, temperature, ionic strength, etc.).[50−52] When applied to large-scale adsorption systems, the mode of contact between the adsorbate and adsorbent is also important to consider. Batch adsorption (static method) and fixed-bed adsorption (dynamic method) are two of the most widely used adsorption methods and are briefly discussed in the next section.

While many models (Langmuir, Freundlich, Temkin, Redlich-Peterson, Dubinin−Radushkevich−Kaganer [D-R-K], Dubinin−Radushkevich [D-R]) have been designed to fit isotherm data,[34] the two most commonly applied models (Langmuir and Freundlich isotherm models) have been satisfactory in describing the adsorption process in most studies clearly evident from Table 2 also lists important experimental characteristics, including the adsorption model, initial phosphate concentration, temperature, pH, and resulting adsorption capacity. While some adsorbent materials described in Table 2 have large adsorption capacities, most corresponding adsorption studies have been conducted using synthetic solutions. The effect of specific parameters on the adsorption characteristics is further discussed in section 2.4.

2.1. Adsorbents

The most important factor for phosphate adsorption is identifying an ideal and efficient adsorbent. The adsorbent should possess high selectivity, high adsorption uptake capacity (preferably porous, leading to high surface area), longevity, be available in large quantities, and be reusable, cost-effective, biodegradable, and biocompatible.[33,34,70] Various factors such as the adsorbate structure, particle size, surface charge, porosity, and surface area influence the adsorbent characteristics, while water solubility, hydrophilicity, charge, and molecular weight affect the adsorbate properties. Recently, Du et al. critically reviewed the synthesis methods and modification strategies for various adsorbents to enhance phosphate adsorption capacity and selectivity.[71] Numerous reactive media have been developed for phosphate removal, which include:

- *Natural materials*, including marble dust, sawdust, soil, and rice[70,72]
- *Minerals*, including zeolites,[73,74] opoka,[75] bentonite,[76] hydroxy-aluminum pillared bentonite,[77] calcite,[78] dolomite,[79] gibbsite,[80] sepiolite,[80] La-modified tourmaline,[63] and layered double hydroxides[81]
- *Industrial byproducts*, including fly ash,[82−84] bottom ash,[85] red mud,[86] slag,[87−89] modified steel slag,[87] alum sludge,[88] skin split waste,[89] sludge,[90] and iron oxide tailing[42]
- *Composite adsorbents* such as binary Fe−Mn binary oxide,[65] tertiary-metal Fe−Mg−Al composites,[15] Ce−Zr binary oxide,[67] Fe−Ti bimetal oxide,[68] Fe−Zr binary oxide,[91] and Fe−Cu binary oxide[6]
- *Adsorbents as nanoparticulates* such as ferrihydrite nanoparticles and zirconium oxide nanoparticles[1,92]
- *Polymeric adsorbents* such as Duolite C 466,[93] chitosan,[94] and polypropylene-*g*-*N*,*N*-dimethylamino ethyl methacrylate[50,93]
- *Magnetic adsorbents* such as amine functionalized silica magnetite,[95] magnetic Fe_3O_4@C@ZrO_2,[96] and magnetic Ca and Mg modified iron oxide[57]
- *Modified and unmodified carbonaceous materials*[97] including *undoped*[26,98] and *metal-doped* activated carbon,[26,99,100] CNTs, graphene,[101] graphene oxide, graphite, graphite oxide, charcoal, carbon nanofibers as well as unmodified and modified biochar[102,103]
- *Bioadsorbents* such as oyster shell,[30] eucalyptus,[104] palm surface fiber,[25] okara,[105] wood particles,[106] wheat residue,[107] and fruit juice residue[44]
- *Metal oxide/hydroxide* such as aluminum oxide,[32] lanthanum oxide,[32] lanthanum hydroxide,[45] and Bayoxide (B33)[49]
- *Building waste* from demolition of buildings (e.g., bricks and cement) rich in magnesium, iron, calcium, and aluminum[31]

2.2. Characterization of Synthesized Adsorbents for Phosphate Recovery

Surface morphologies of the adsorbents, both before and after phosphate adsorption, have been examined using scanning electron microscopy (SEM) and transmission electron microscopy (TEM). In addition, X-ray diffraction (XRD) has been used to determine the composition and quality of the adsorbent's crystal structure, energy dispersive X-ray spectrophotometry (EDX) has been used for elemental analysis of the adsorbents, and BET analysis to extract specific surface area. Fourier transform infrared (FTIR) spectroscopy has also been used to investigate the adsorption mechanisms at the adsorbent surfaces.

2.3. Assessment of Adsorption Capacity

The adsorption characteristics of different adsorbates used for phosphate recovery are summarized in Table 2, along with their experimental conditions (i.e., pH and temperature) and adsorption method. From the table, it can be observed that most adsorption studies were performed via a batch method to examine the adsorption mechanism. Additionally, the Langmuir model was the best fit for most adsorption isotherm data. Other characteristics, such as the effect of adsorbate features (e.g., porosity, chemical nature, surface modification, etc.), pH, temperature, and coexisting ions on the capacitive nature of different adsorbents, are discussed in detail in the upcoming sections.

2.3.1. Effect of Adsorbate Characteristics. Several adsorbent characteristics greatly influence the adsorbent's performance. The porosity and available surface area are among the most important features for estimating the adsorption capacity of the adsorbent.[108] Additionally, metal

https://doi.org/10.1021/acsenvironau.3c00069
ACS Environ. Au 2024, 4, 271−291

doping, chemical or acid treatment, surface modification, ligand adsorption, and ion-exchange capacity are some of the other parameters that can be experimentally modulated to optimize the adsorption capacity. Several researchers have investigated these parameters in the context of phosphate adsorption and are discussed below.

Xue et al. reported that acid treatment of adsorbents, such as basic oxygen furnace slag, increases the porosity and surface area of the adsorbent and enhances phosphate adsorption (~20%) due to the enlargement of aperture diameter and formation of micropores.[48] On the other hand, Wang et al. examined and compared the phosphate adsorption of pure ferrihydrite (FH) and complexes of ferrihydrite and humic acid (FH-HA) and found that the specific surface area in pure FH (368.2 m^2/g), FH-HA1 (321 m^2/g), and FH-HA2 (114.3 m^2/g) decreased with an increase in humic acid, which led to a decrease in adsorption capacity.[109] Yan et al. investigated several bentonite systems and found their specific surface areas to be as follows: hydroxy-aluminum pillared bentonite (Al-Bent, 200 m^2/g) > hydroxy-iron pillared bentonite (Fe-Bent, 143 m^2/g) > hydroxy-iron−aluminum pillared bentonite (Fe−Al−Bent, 94.9 m^2/g), as measured by BET. The adsorption capacity also followed the specific surface area trend with the following values: Al-Bent (5.05 mg/g) > Fe-Bent (4.84 mg/g) > Fe−Al−Bent (4.64 mg/g), confirming a correlation between surface area and adsorption capacity.[77]

Lalley et al. modified the surface of Bayoxide E33 with nanostructured Ag and Mg and compared the adsorptive properties to unmodified E33. The adsorption capacity at pH 7, as predicted by the Langmuir isotherm, for modified and unmodified Bayoxide E33 is shown in Figure 2. Here, it was

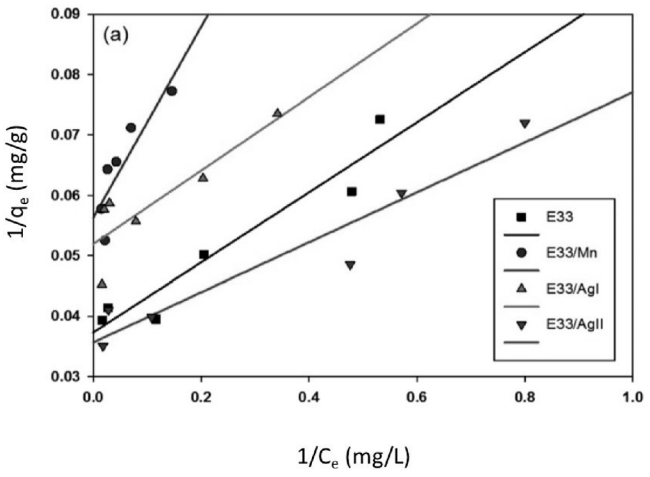

Figure 2. Langmuir isotherm graphs at pH 7. Adapted with permission from Lalley et al.[69] (Copyright 2015 Royal Society of Chemistry).

found that the BET surface area correlated well with the adsorption capacity in the following order : E33/AgII (142 m^2/g: 28.0 mg/g) > E33 (140 m^2/g: 26.3 mg/g) > E33/AgI (124.6 m^2/g: 19.3 mg/g) > E33/Mn (102.8 m^2/g: 17.8 mg/g).[69]

In another study, Martin et al. developed porous metal carbonate-based adsorbing structures to remove phosphate and ammonia from various aqueous media.[55] Powdered magnesium carbonate, which has a very low water solubility (i.e., 0.1 g/L at 25 °C), was mixed with a cellulose binder and pressed into structures, which were then calcined. These magnesium carbonate structures (i.e., pellets) were nanoporous with a high surface area, resulting in high water permeability and surface area available for loading. These $MgCO_3$-based pellets recovered over 80% of 160 mg/L ortho-phosphate in deionized water. In addition, the average sorption capacity achieved was 97 mg of P per gram of $MgCO_3$ based on sorption isotherm studies. Desorption tests in deionized water, 0.1 M HCl, or 0.1 M NaOH suspensions showed that the leaching of P into aqueous suspensions (pH 4−10) was <4.5% of the adsorbed-P for 25 days, indicating a great application potential as a slow-release material.

While zeolites have been extensively used for wastewater treatment, they are rarely used for phosphate removal as they carry negatively charged anions on the surface. Therefore, for phosphate removal, zeolites are often modified with different metal oxides to improve the ionic exchange capacity.[110] Guaya et al. modified natural zeolites with hydrated aluminum oxide for phosphate removal and showed a significant increase (0.6 mg/g to 7.0 mg/g) in phosphate sorption on the modified zeolite surface.[74] Choi et al. investigated the adsorption behavior of natural zeolite (hydrated aluminosilicate), hydrotalcite, and activated alumina surfaces and their sulfate-coated counterparts toward phosphate removal. In their study, the authors found that sulfate-coated zeolites showed higher adsorption capacity compared to alumina and hydrotalcite, especially natural zeolite, which showed an increase from 3.59 mg/g to 58.89 mg/g and 4.70 mg/g to 111.49 mg/g in pellet and powder form, respectively when coated with sulfate.[46]

Grafting (as a surface modification) on polymeric matrices (hollow fiber, nonwoven fabric, film) followed by their functionalization is often employed to enhance adsorption capacity.[50] Besides surface modification, specific affinity toward phosphates due to the intrinsic chemical nature of the adsorbent is also important. For example, oxides and hydroxides of metals such as Fe(III), Zr(IV), Al, Mn, Ti, and Cu(III) have been repeatedly explored for phosphate removal as they exhibit strong ligand adsorption (of HPO_4^{2-} and $H_2PO_4^-$) by forming inner-sphere complexes via Lewis acid−base interactions.[111] Acelas et al. prepared hydrated immobilized ferric oxide (HFeO), hydrated zirconium oxide (HZrO) and hydrated copper oxide (HCuO) within a microporous anion exchange resin (IRA-400). The results revealed that the hybrid systems had a greater affinity toward phosphate removal than base-only resins. The Fe−Zr hybrid materials were more selective and effective for synthetic and real solutions and removed 83% and 86% of phosphate, respectively.[112] Zirconium-based adsorbents such as Zr-oxide, ferrites, sulfates, and hydroxides have also shown a strong affinity for phosphate.[111] For example, amorphous zirconium-oxide nanoparticles were synthesized by Su et al. using a hydrothermal method and found the phosphate adsorption capacity to be 99.01 mg/g at pH 6.2.[1]

Composite adsorbents (containing two or more different metal oxides) for phosphate removal are also important as they possess the features of their parent metal oxides, and their composite nature synergizes the effect of metal oxides, enhancing their adsorption performance.[6,111] Nanoadsorbents such as nanoscopic metal oxides have also exhibited effective phosphate adsorption due to their large specific surface areas.

Nanostructured Fe−Cu binary oxides were synthesized via a facile coprecipitation process by Li et al.[6] They suggested that inner-sphere surface complexes were formed by phosphate anions at the water/oxide interface, leading to a maximum adsorption capacity of 39.9 mg/g at pH 4. Su et al. synthesized Ce−Zr binary oxides nanoadsorbents by solvothermal proc-

https://doi.org/10.1021/acsenvironau.3c00069
ACS Environ. Au 2024, 4, 271−291

ess.[67] The phosphate adsorption capacity of $Ce_{0.8}Zr_{0.2}O_2$ nanoparticles was found to be 112.23 mg/g. Here, the adsorption followed the inner-sphere complex mechanism, and the surface−OH groups also played an important role. Chen et al. used nanocomposite adsorbent HZO-201 based on nanohydrous zirconium oxide (HZO) for phosphate removal from water. Here, an anion exchange resin (D-201) was employed as the host of HZO-201, as shown in Figure 3. As the

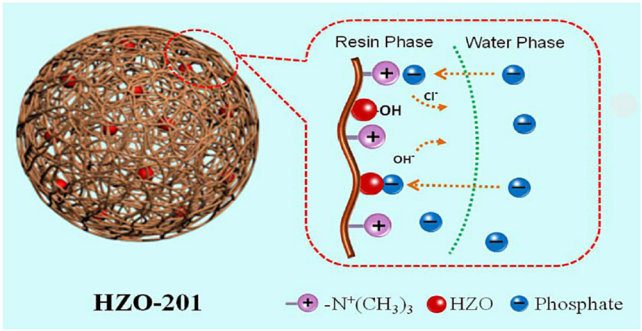

Figure 3. Schematic illustration of HZO-201 (nanoscopic hydrated zirconium oxide within polymeric anion exchanger D-201) and its phosphate adsorption. Adapted with permission from Chen et al.[111] (Copyright 2015 Elsevier).

figure schematically depicts, the binding of phosphate to D-201 was attributed to a nonspecific electrostatic affinity. In contrast, the phosphate adsorption on loaded HZO nanoparticles was attributed to forming inner-sphere complexes.[111] Similarly, Hua et al. immobilized nanosized HFO (hydrated ferric oxide) within D-201 to remove phosphate from effluent discharged from municipal wastewater.[113]

Most clay minerals, such as montmorillonite, zeolite, kaolinite, and mica, carry negative charges that hinder the adsorption of phosphate ions onto their surfaces. Thus, several researchers have focused on another type of clay mineral called layered double hydroxides (LDHs), or hydrotalcite, which has positive charges. These minerals are composed of positively charged brucite-like sheets with intercalated anions in the hydrated interlayer regions to balance the positive charges. LDHs are used as adsorbents due to their high anionic exchange capacity.[36,77,114] Yu et al. synthesized pyromellitic acid intercalated ZnAl-LDHs (Zn_2Al-PMA-LDHs) and reported high selectivity (97.41% at pH 7.0) toward phosphate ($H_2PO_4^-$ and HPO_4^{2-} anions). This high adsorption capacity was attributed to the formation of hydrogen bonds between the phosphate −OH groups (donor) and the oxygen of the dissociated carboxyl group of pyromellitic acid (acceptor).[12] In another study, three different magnetic core−shell Fe_3O_4@LDHs nanoparticles (Fe_3O_4@Zn−Al−, Fe_3O_4@Mg−Al−, and Fe_3O_4@Ni−Al-LDH) were prepared by Yan et al. for phosphate adsorption. This study found the adsorption capacity to follow the order:Fe_3O_4@Zn−Al-LDH (37 mg/g) > Fe_3O_4@Mg−Al-LDH (32 mg/g) > Fe_3O_4@Ni−Al-LDH (26 mg/g).[81] Novillo et al. synthesized Mg/Al LDH (2:1) and found the optimum adsorption capacity to be 71.2 mg/g under acidic conditions of pH 3. Under these conditions, it was interpreted that acidic pH led to the release of Al and Mg from the LDHs sheets into the solution, effectively working as precipitating agents and eliminating phosphates from the solution.[36]

Other good substrate materials for the removal of phosphate include ordered mesoporous silica doped with various transition metals (e.g., Fe, Zr, Al, Ti) and lanthanide oxides due to their controlled pore size, morphology, high surface area, nontoxic nature as well as their environmental friendliness.[114,115] In one study, Delaney et al. modified mesoporous silica with metal oxides (i.e., Zr, Al, Fe, and Ti) to remove phosphates. These researchers compared the affinity with undoped mesoporous silica at different temperatures, pH, and molar ratios.[115] They reported that undoped mesoporous silica has little or no bonding affinity for phosphate removal. However, metal-doped oxides grafted on mesoporous silica surfaces were found to be very effective adsorbents, where phosphate removal reached 100% under certain experimental conditions and were rationalized via an equilibrium limited adsorption process, where phosphate species were weakly bound to the substrate.

2.3.2. Effect of Coexisting Anions. Several anions such as NO_3^-, SO_4^{2-}, Cl^-, and HCO_3^- are known to coexist with phosphate anions in wastewater, which can evidently interfere with phosphate removal efficiency through competition for adsorption sites with phosphate ions on the adsorbent surface.[40,100,116] Deng et al. studied phosphate removal at pH 7.5 using Mg−Al hydrotalcite loaded kaolin clay, and observed that phosphate adsorption decreased in the order of SO_4^{2-} > NO_3^- > Cl^- ions, where the removal efficiency decreased from 92% to 66%, 96 to 86%, and 98% to 89%, respectively, for the three anions.[7] Anirudhan et al. examined the adsorption of phosphate onto amine functionalized epichlorohydrin-grafted cellulose (Cell-g-E/PEI) at pH 4.5 and showed that the inhibition of coexisting anions on phosphate adsorption follows this order: HPO_4^{2-} > SO_4^{2-} > Cl^- > NO_3^-.[117] In both studies, it was suggested that nitrate and chloride ions have a relatively minor impact on phosphate adsorption because both anions only form an outer-sphere complex and thus are unable to compete well with phosphate. In contrast, sulfates form both outer and inner sphere complexes with the surface active sites and, thus, can compete with phosphate to a better degree.[7,117] In another study, Novillo et al. found the order to be NO_3^- > HCO_3^- > Cl^- > SO_4^{2-} while studying the effect of coexisting anions on the Mg/Al LDH adsorbents at pH 3.[36] In comparison with the pure phosphate solution, the percentage of adsorbed phosphate on Mg/Al LDH was found to be higher in the presence of nitrate and bicarbonate ions, but lower in the presence of SO_4^{2-}. This observation was attributed to the higher affinity of the LDH toward divalent anions (SO_4^{2-}) compared to monovalent ions ($H_2PO_4^-$ at pH 3).

Several studies have reported minimal or no influence of coexisting ions on the efficiency of phosphate adsorption. Su et al. examined the effect of coexisting anions on phosphate adsorption for amorphous ZrO_2 nanoparticles at two different concentrations (5 and 10 mM). It was observed that the presence of SO_4^{2-}, Cl^- and HCO_3^- ions, even at very high concentrations (as compared to the concentration of phosphate ions), had no or a slight effect on phosphate adsorption.[1] Song et al. reported a similar effect with SO_4^{2-} and Cl^- ions having no significant effect on phosphate adsorption onto ferric sludge.[8] Guaya et al. used natural zeolite rich in clinoptilotite modified by incorporating hydrated aluminum oxide for phosphate removal. In this study, HCO_3^- reduced the phosphate uptake by 32% while other competing ions did not compete for the same binding sites.[74] Other authors (Huang et al.[10,29] and Liu et al.[40,118]) have also reported that coexisting anions had small effects on phosphate removal efficiency for composite metal oxides (manganese ore tailing) (CMOMO),[118] $La(OH)_3$-modified exfoliated vermiculites,[29] ferric-modified laterites,[10]

https://doi.org/10.1021/acsenvironau.3c00069
ACS Environ. Au 2024, 4, 271−291

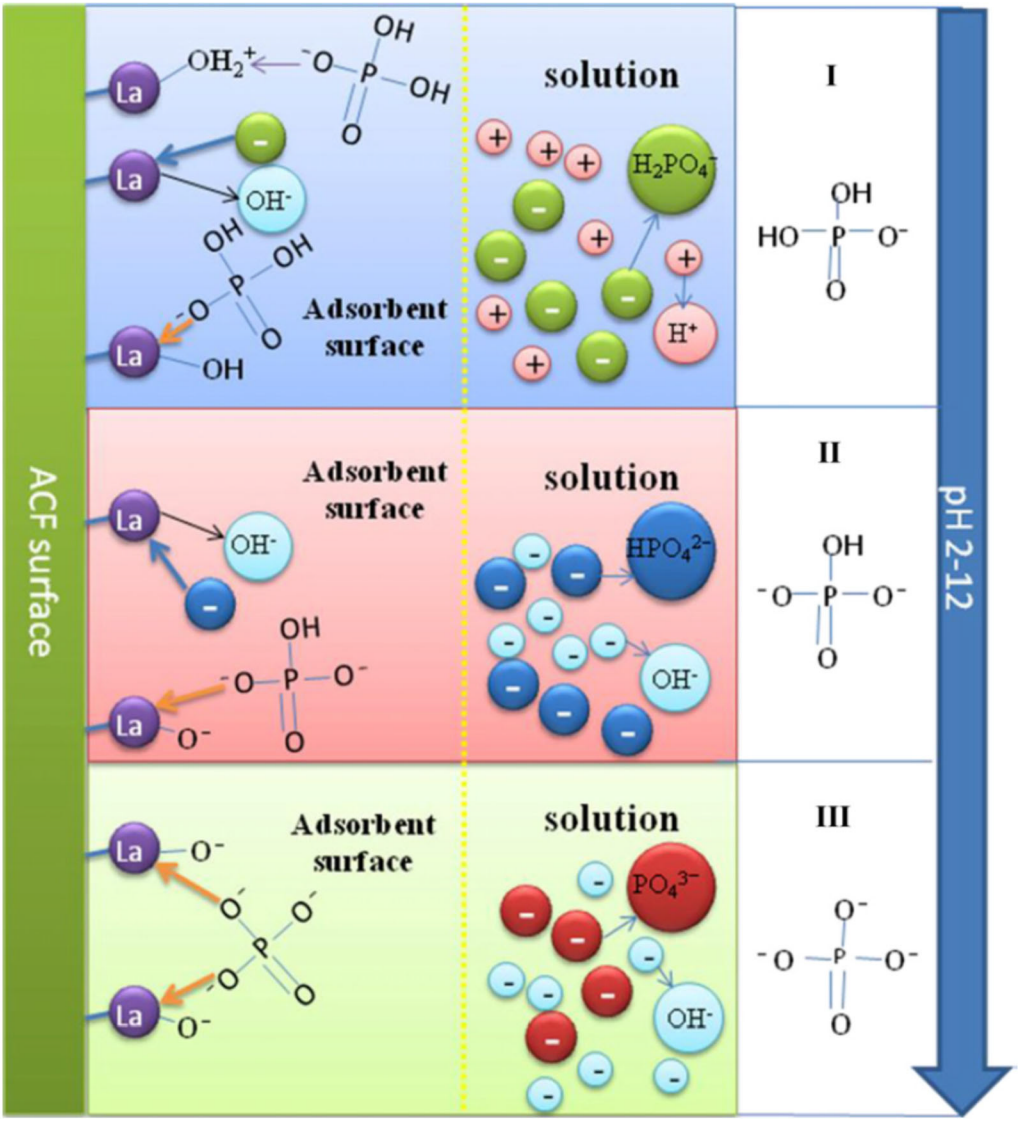

Figure 4. Mechanism of phosphate adsorption on lanthanum hydroxide-doped activated carbon fiber (ACF-LaOH) at different pH values of the medium. Adapted with permission from Zhang et al.[99] (Copyright 2012 Elsevier).

and hydroxyl-iron−lanthanum doped activated carbon fiber (ACF-La).[40]

2.3.3. Effect of pH. Phosphate anions are known to adsorb via a ligand exchange process, where chemical interactions and electrostatic forces play an important role.[119,120] In solution, the pH plays a crucial role in the adsorption of phosphates due to modulation of these interactions. pH governs the phosphate dissociation equilibria in the solution, affects the strength of electrostatic attraction, and determines which phosphate species are dominant at a certain pH. The dissociation of phosphates at different pH regimes is expressed below:[95]

$$[H_3PO_4] \leftrightarrow [H^+] + [H_2PO_4^-] \quad pK_1 = 2.12$$

$$[H_2PO_4^-] \leftrightarrow [H^+] + [HPO_4^{2-}] \quad pK_2 = 7.21$$

$$[HPO_4^{2-}] \leftrightarrow [H^+] + [PO_4^{3-}] \quad pK_3 = 12.67$$

PO_4^{3-} predominates in strong basic conditions, HPO_4^{2-} predominates in weak basic conditions, and $H_2PO_4^-$ and H_3PO_4 predominate in weak and strong acidic conditions. In addition to pH, pH_{pzc} (i.e., pH at the point of effective zero charge on the adsorbate) also plays an important role in the adsorption process. If pH < pH_{pzc}, the surface charge is positive leading to an increase in phosphate adsorption due to attractive electrostatic interactions. When pH > pH_{pzc}, the surface charge of adsorbents becomes predominantly negative, leading to a lower phosphate adsorption. Furthermore, an increase in pH also leads to the formation of OH^- ions that occupy more active sites on the surfaces of the adsorbents and induce the formation of a new counter-charged ion layer that decreases phosphate adsorption.[50,100,121]

Zhang et al. proposed a mechanism of phosphate uptake on LaOH-doped activated carbon fibers at different pHs, as shown in Figure 4.[99] A decrease in the adsorption behavior was observed with an increase in pH. At lower pH (2−8), ligand exchange was identified as the main contributor toward adsorption capacity. At low pH, a positively charged surface group (OH_2^+) was found to be more displaced from the metal binding sites than hydroxyl groups, facilitating the ligand exchange process. The ligand exchange process decreased with increasing pH (>10), leading to a very low adsorption capacity. High pH values caused the surface to carry more negative

https://doi.org/10.1021/acsenvironau.3c00069
ACS Environ. Au 2024, 4, 271−291

charges, resulting in an increased repulsion between the negatively charged surface sites and the more negatively charged PO_4^{3-} species.

Chiou et al. reported that the adsorption capacity of magnetite-modified diethylenetriamine for phosphate species increased with a decrease in pH up to a pH = 3 and was attributed to the protonation of amine groups on the magnetite adsorbent. This study noted that at pH_{zpc}, which was acidic, further decreases in pH led to protonation of the adsorbate. This resulted in little adsorption, as under such acidic conditions, the phosphate is either in neutral (H_3PO_4) or weakly ionized form ($H_2PO_4^-$).[95] Song et al. observed that the maximum adsorption capacity (>10 mg/g) occurred between pH 4 and 6, with adsorption values decreasing when deviating from this pH range during phosphate adsorption on ferric sludge.[8] At a low pH, the surface hydroxyl groups were protonated and easily replaced at the binding sites, while at a higher pH, the surface became more negative, reducing phosphate adsorption. Shanableh et al. tested six Al, Fe, and Al−Fe-modified bentonite adsorbents to remove phosphate from water.[122] It was found that the pH affected the phosphate adsorption capacities with optimal adsorption at pH = 5 (8.9−14.5 mg/g). Adsorption decreased by approximately 37% when the pH increased from 5 to 8. Yan et al. investigated the adsorption capacity of calcined alkaline residue AR800 for phosphate removal,[123] noting an increase from 35 to 55 mg/g as pH rose from 2.5 to 5.5. However, the adsorption capacity dropped to 40 mg/g with further increase in pH. Karageorgiou et al. used calcite adsorbent for phosphate removal and examined the effect of pH from 7 to 12.[124] Unlike previous studies, orthophosphate uptake was comparatively lower in the slightly basic pH region (approximately 70−80%), but increased significantly, achieving complete uptake near pH 12.

2.3.4. Effect of Temperature and Thermodynamic Nature. The thermodynamic nature of phosphate adsorption is often characterized by determining the thermodynamic equilibrium constant (K_d) at various temperatures. The change in enthalpy (ΔH), entropy (ΔS), and free energy (ΔG) are estimated from the slope and intercept of the ln K_d vs $1/T$ plot, respectively. Thermodynamic factors of the adsorption process, such as spontaneous or non-spontaneous and exothermic or endothermic, along with changes in enthalpy (H), Gibbs free energy (G), and entropy (S) of the adsorption are determined by the following equations:[7,77]

$$\Delta G = \Delta H - T\Delta S$$

$$\ln K_L = -\frac{\Delta G}{RT} = -\frac{\Delta H}{RT} + \Delta S/R$$

where K_L (L/mol) is the Langmuir constant associated with temperature. Several authors have reported that an increase in temperature has a positive effect on the phosphate uptake (increased K_L), and thus, making temperature an important factor in phosphate adsorption.[12,41,65,93,125−128]

Jutidamrongphan et al. reported an increase in phosphate adsorption onto silica sulfate increased as temperature increased from 15 to 45 °C at pH 6.5.[61] The thermodynamic parameters showed that the adsorption process consisted of chemisorption and physical adsorption, was endothermic in nature (positive ΔH), spontaneous, and demonstrated a good affinity of phosphate ions toward the adsorbent with increased randomness (positive ΔS) at the solid-solution interface. Yang et al. investigated the effect of temperature on phosphate adsorption by a tablet porous material (TPM) and found that phosphate removal increased when the temperature increased from 14 to 34 °C.[129] Similarly, phosphate removal was observed to be spontaneous and endothermic, where an increase in temperature enhanced the binding tendency of phosphate to the interface between TPM and phosphate. Similar trends have been observed in the removal of phosphate using many other adsorbents inlcluding core−shell Fe_3O_4 LDHs,[81] chitosan beads modified with zirconium ions,[11] lanthanum doped activated carbon fiber,[26] pyrrhottite,[125] and TEPA-Fe_3O_4-NMPs.[127]

Several authors have noted a decrease in adsorption capacity with temperature, attributing it to an exothermic nature (negative ΔH).[7,16,29,63] For example, Paleka et al. found that the sorption capacity decreased (from 34.57 to 13.85 mg/g) with an increase in temperature from 25 to 65 °C for aluminum oxide S.[16] In the study, the sorption of phosphates onto aluminum oxide S was observed to be an exothermic process (enthalpy ΔH = −48.7 kJ/mol), suggesting that the adsorption process was chemisorption. Similarly, Yuan et al. reported that phosphate adsorption decreased when temperature increased from 20 to 80 °C on dolomite, and the phosphate adsorption was exothermic (enthalpy ΔH = −5.85 kJ/mol).[130] Similar trends were also observed on rice husk and fruit juice residue,[44] as well as La-modified tourmaline.[63]

2.3.5. Effect of Calcination. To realize the maximum adsorption efficiency of different adsorbates, experiments have been conducted on adsorbates calcined at varying temperatures. For example, as shown in Figure 5, Akar and co-workers

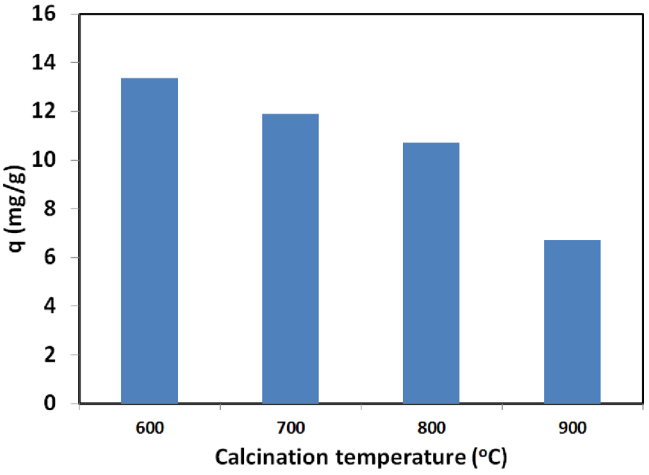

Figure 5. Effect of calcination temperature on the phosphate adsorption capacity of TDPA-KCl (conditions: initial phosphate conc.: 50 mg/L; pH: 3.0; adsorbent: 2.0 g/L, t: 60 min). Adapted with permission from Akar et al.[51] (Copyright 2010 Elsevier).

demonstrated that the adsorption of phosphate ions on alunite ore-KCl adsorbent decreased with an increase in calcination temperature (after 650 °C) due to the partial sintering of alunite.[51] For Zn−Al LDHs, the most phosphate uptake (40.77 mg/g) was observed when the adsorbent was calcinated at 300 °C by Cheng et al.[52] Here, the adsorption capacity was found to be 1.55-fold higher than that of the uncalcined material. Furthermore, unlike Akar et al., the phosphate adsorption capacity exhibited a nonmonotonic behavior with respect to calcination temperature. The adsorption capacity modestly increased for calcination temperatures from 150 to 300 °C, following by a slight decrease up to a temperature of 500 °C, and then a substantial decrease at higher temperatures (>500 °C).

https://doi.org/10.1021/acsenvironau.3c00069
ACS Environ. Au 2024, 4, 271−291

Similar results (i.e., nonmonotonic behavior) were obtained when fly ash (optimal adsorption of 6.59 mg/g @ 800 °C)[83] and red mud (optimal adsorption of 19.1 mg/g @ 700 °C)[56] were used as phosphate adsorbents. For the latter study, it was suggested that during calcination, water removal leads to greater porosity and, thus, a higher surface area. For calcined temperatures greater than the optimal temperature, the decrease in phosphate removal was attributed to the decomposition of some hydroxyl groups, calcite, and the sintering shrinkage of red mud.[56] Peleka et al. reported that between calcination of hydrotalcite at 400 °C and 500 °C, the higher temperature showed approximately 25% larger sorption capacity (244.58 mg/g@500 °C vs 192.9 mg/g@400 °C) at room temperature.[16]

2.4. Mechanisms

The mechanism of phosphate adsorption depends on the surface characteristics (physical and chemical features) of the adsorbent and is indicative of the capacity, energy, and kinetics of the adsorption phenomenon.[7,51,81,131] The mechanism provides meaningful insights into adsorption and subsequent desorption and regeneration processes, and can optimize the adsorption capacity. Based on the type of molecular interactions, the mechanism of adsorption can be broadly categorized based on physical or chemical adsorption characteristics, and it is briefly summarized below.

2.4.1. Ion Exchange. Ion exchange interaction is a type of molecular interaction in which a counterion on the adsorbent's surface is replaced by a chemically equivalent number of another counterion (i.e., the ion in solution is adsorbed while the attached ion on the adsorbate's surface is desorbed). It is a stoichiometric process that maintains the electroneutrality of the solution. It is also referred to as "outersphere" surface complexation as the exchanging ions reside in the *outer sphere* (2nd coordination shell) of the metal coordination complex,[132] fully retaining their inner hydration shell (see Figure 6a). These interactions are dominated by electrostatics and are, thus, reversible in nature.[11,111] In the context of phosphate adsorption, phosphate anions are physically adsorbed in this mechanism, replacing other anions, such as chlorides, sulfates, and bicarbonates, from the outer sphere surface. Several authors have reported ion exchange as the possible mechanism for phosphate adsorption on many adsorbents, such as anion-exchange resins,[132,133] polymer-based nanosized hydrated ferric oxides (HFOs),[134] modified chitosan with zirconium ion,[11] etc.

2.4.2. Ligand Exchange. Unlike ion exchange, ligand exchange involves the formation of chemical bonds between the adsorbate and incoming phosphate ion. Due to its chemical nature, it is considered a fast, strong, and often irreversible process. In this process, phosphate ions replace hydroxyl ions attached to the metallic surface via "innersphere" complex formation (see Figure 6b).[8,9,25,66] Here, the inner sphere refers to the hydration shell of the metal coordination complex, involved in ligand exchange. In this mechanism, as the adsorbed phosphate anions add negative charge on the surface, the point of zero charge is shifted to lower pH values. In addition, the desorbed OH anions increase the pH of the solution.[114] The presence of these features often indicates of ligand-exchange as the possible mechanism for phosphate adsorption, which is also often characterized by the pseudo-second-order kinetics of adsorption. Many different adsorbents, such as lanthanum modified adsorbents,[29] La-ACF, polymer ligand exchangers, hydrated aluminum oxide modified zeolite,[74] hydrated metal oxides,[112] ferric modified laterites,[10] and basic oxygen furnace slag,[120] have been reported to follow this mechanism for phosphate adsorption.

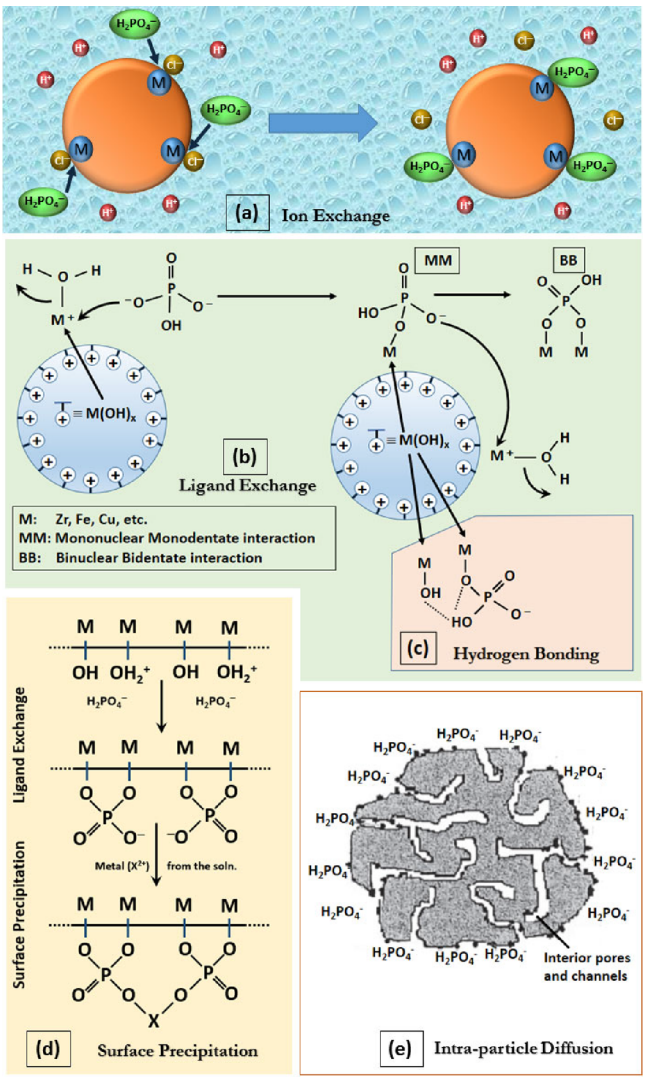

Figure 6. Schematic representation of different adsorption mechanisms. (a) ion-exchange; (b) ligand-exchange; (c) hydrogen-bonding; (d) surface precipitation; and (e) diffusion.

2.4.3. Hydrogen Bonding. Loganathan et al. have suggested that hydrogen bonding also plays a role in determining phosphate adsorption characteristics.[114] In the context of phosphate adsorption, hydrogen bonding, a dipole−dipole interaction, occurs when a strong electropositive hydrogen atom bonded to a strongly electronegative atom (such as H in OH of metal oxides) interacts with the electronegative oxygen atom of chemically adsorbed phosphate anions.[114] This interaction could be considered an auxiliary mechanism to ligand-exchange, where innersphere hydration atoms of the metal complex are involved in H-bond formation with previously adsorbed phosphates (see Figure 6c). This interaction is noted to be weaker than chemical ligand-exchange interactions but stronger than physical ion-exchange interactions.[114]

2.4.4. Surface Precipitation. While surface complexation, as described by a ligand-exchange mechanism, is an important adsorption mechanism to describe phosphate adsorption, several studies have indicated that surface reaction for phosphate is often more complex. In many cases, further deposition of

https://doi.org/10.1021/acsenvironau.3c00069
ACS Environ. Au 2024, 4, 271−291

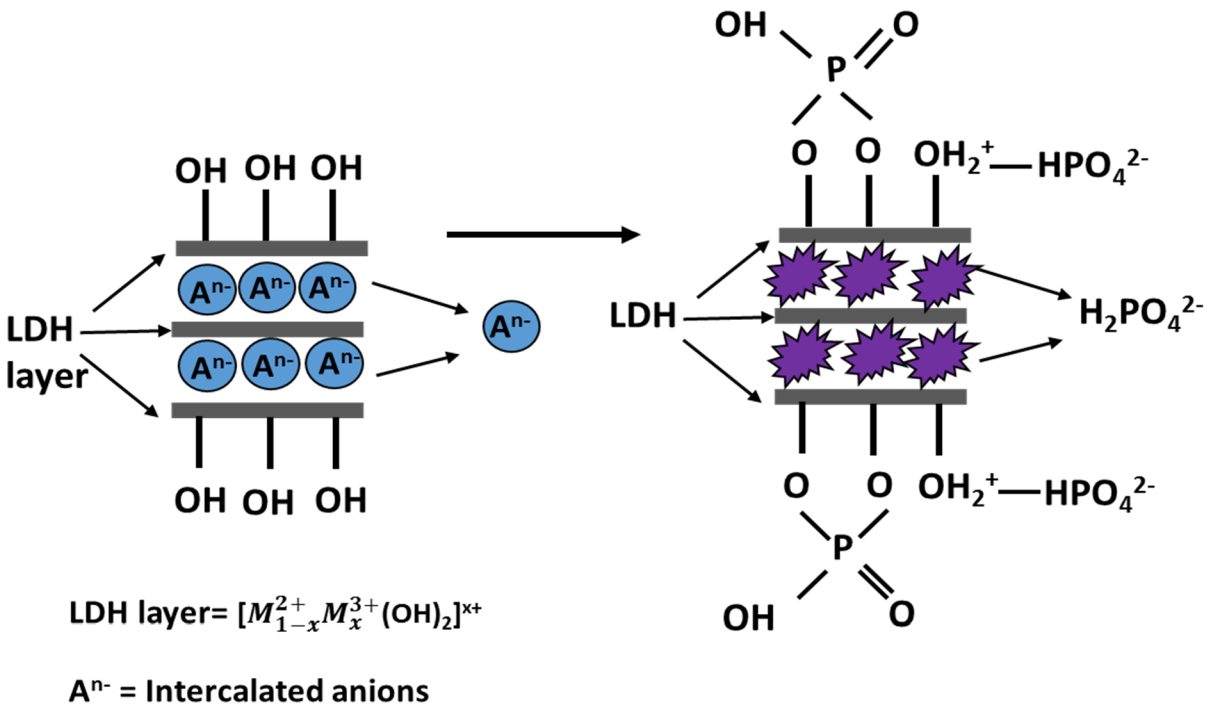

Figure 7. Schematic representation of the intercalation mechanism.

cations (from solution) on previously adsorbed phosphates forms precipitates of metallic phosphates on the surface of the adsorbent—a phenomenon commonly known as surface precipitation (see Figure 6d). It has also been suggested that the monolayer deposition of phosphate ions transitions to multilayer deposition.[66] This can occur even at low concentrations of phosphate and metallic ions, where precipitation is not thermodynamically feasible in the solution. in such cases, a finite volume exists near the adsorbent surface that is oversaturated interms of precipitate formation.[114] As the multilayer formation can begin without prior saturation of monolayer adsorption, it becomes extremely difficult to accurately predict the onset of surface precipitation as both surface complexation and surface precipitation can coexist during phosphate adsorption. In literature, when adsorption is best characterized by the Freundlich isotherm, observing a linear regime is attributed to the existence of surface precipitation.[135] Recently, changes in zeta potential as a function of the amount adsorbed have also been identified as an important parameter to delineate adsorption and surface precipitation mechanisms.

2.4.5. Diffusion. Diffusion of phosphate ions on adsorbents has also been treated as an adsorption mechanism,[114] but it appears to be more indicative of adsorption kinetics. For many types of adsorbents, such as hydrous metal oxides and porous adsorbents, phosphate diffusion is regarded as a two-step process often termed film diffusion (fast process) and intraparticle diffusion (slow process).[114] The fast process refers to the quick initial adsorption of phosphates on the adsorbent surface reaching a pseudoequilibrium, while the slow process refers to the diffusion of phosphate ions into the hard-to-reach pores/channels/cavities[136] within the adsorbent (referred to as intraparticle diffusion), as shown in Figure 6e. Since the earlier stages of adsorption (fast diffusion) are often controlled by the mass deposition rate, it is also called mass transfer controlled adsorption. Similarly, the long-time kinetics (slow diffusion) is referred to as diffusion-controlled adsorption, as the adsorption is limited by diffusion characteristics of adsorbed phosphate ions.[137]

2.4.6. Intercalation. Adsorption via intercalation is often exhibited by layered double hydroxides (LDHs), which, due to their relatively weak interlayer bonding, exhibit a desirable ability to capture organic and inorganic anions (Figure 7). LDHs are represented by the general formula $[M_{1-x}^{2+}M_x^{3+}(OH)_2]^{x+}(A^n)_{x/n}.mH_2O$, where, x normally ranges from 0.17 to 0.33, M^{2+} is a divalent cation (Zn^{2+}, Ni^{2+}, Mg^{2+}, Mn^{2+}, or Cu^{2+}), M^{3+} is a trivalent cation (Cr^{3+}, Fe^{3+}, or Al^{3+}), while A^{n-} corresponds to the incorporated anions (organic, inorganic, oxoanion, carboxylate, polyoxometalates, and coordination compounds) residing within the interlayer region along with water molecules for structural stability and charge neutrality.[12,36,52] The molecular structure of LDHs consists of positively charged brucite-like sheets, which are complemented by intercalated anions in the hydrated interlayer regions. Here, a positive charge is developed on the layer due to the partial substitution of trivalent cations for their divalent counterpart. LDHs possess intrinsic anion uptake capacity due to the presence of facile exchangeable interlayer anions, large available surface area for adsorption, and high charge density, and hence have been explored in detail for the removal of phosphate from contaminated water.[81,135,138] A series of layered double hydroxides (LDHs) with different metal cations such as Zn/Al LDH,[52] Zn/Al/Zr LDH,[135] Mg/Al LDH,[36] and core−shell Fe_3O_4@LDHs.[81] have been reported for phosphate adsorption.

2.5. Potential for Phosphate Recovery

While significant efforts have been made in developing adsorbent materials for removing phosphate, there is still limited information on the subsequent desorption of nutrients for beneficial reuse within the agricultural sector. The successful desorption of phosphorus from saturated adsorbents has been achieved using alkaline solutions (e.g., 0.01−1 mol/L NaOH), in which the OH^- ions in the NaOH solution (i.e., eluent) exchange with the attached phosphate ions.[139] Bacelo et al.[34]

https://doi.org/10.1021/acsenvironau.3c00069
ACS Environ. Au 2024, 4, 271−291

reported that the desorption efficiency from phosphate-loaded adsorbents typically increased with increasing NaOH solution until an optimum constant level was reached. In several studies, high desorption efficiency was observed (above 80%) using 0.1 mol/L of NaOH as an eluent for a range of adsorbents, including metal hydroxide precipitates,[140] Zr-treated chitosan beads,[11] and metal-loaded activated carbon nanofiber.[141]

In most cases, the direct application of eluate is limited, and phosphate needs to be recovered from the concentrated solutions (containing 380−2530 mg/L of phosphate)[142] via precipitation with calcium or magnesium to be later applied as fertilizers. In one study, struvite was formed by precipitating phosphate using external sources of NH_4^+ and Mg^{2+}, where more than 95% phosphate precipitation was reached after 15 min (see section 4).[142]

The direct use or land application of phosphate-loaded adsorbents is an option for agricultural applications (i.e., direct use as fertilizers). However, soil compatibility and toxicity tests must be conducted for the eventual field application of engineered or biodegradable adsorbents. For example, a series of small-scale controlled environment chamber-based studies can be employed, and measurements of greenhouse gas (GHG) emission (CO_2, CH_4, and N_2O) in headspace and leachates (soluble P, NH_4^+, and NO_3^-) can be conducted in small-scale incubation units. Gas fluxes and leachates indicate soil processes pertaining to soil health, nutrient cycling, and the supply of critical nutrients to plants, indicating the potential use as a fertilizer replacement.

3. CHEMICAL PRECIPITATION METHOD FOR PHOSPHORUS RECOVERY

Chemical precipitation has long been one of the most common ways to remove phosphate. In this process, cationic salts (Fe^{3+}, Al^{3+}, Mg^{2+}, or Ca^{2+}) are added to water containing phosphate. Eventually, insoluble phosphate complexes are formed, followed by their separation from the aqueous phase via sedimentation (sometimes flotation) as precipitates.[143,144] The chemical precipitation method was first described in detail in the 1940s. Chemical precipitates were formed by the reaction of suspended and dissolved phosphate with ferric chloride ($FeCl_3$) or slaked lime ($Ca(OH)_2$). Although lime was one of the main chemicals used for phosphate removal, it is used less frequently today due to the production of sludge and problems associated with handling and storage.[143] Chemical precipitation via crystallization is a phase change process that converts originally dissolved components into an inorganic crystalline particulate or precipitate from the liquid bulk by creating supersaturating conditions (see below) via optimizing experimental conditions (e.g., temperature, pH, and incorporation of external ions).[145]

The reactions involved in the precipitation of phosphate with cationic ions (such as Al^{3+} and Fe^{3+}) are as follows[143]

$$Al^{3+} + PO_4^{3-} \rightarrow AlPO_4 \downarrow$$

$$Fe^{3+} + PO_4^{3-} \rightarrow FePO_4 \downarrow$$

As mentioned above, several metallic cations (Fe^{3+}, Al^{3+}, Mg^{2+} and Ca^{2+}) under different pH conditions have been successful in precipitating phosphates.[16] Mg- or Ca-based precipitation processes have been widely applied to recover and reuse phosphate in the agricultural sector. Recovering phosphate from wastewaters has largely focused on Mg- and Ca-based phosphate precipitates in their crystalline form. These precipitates are respectively known as struvite ($NH_4MgPO_4.6H_2O$) and hydroxylapatite ($Ca_5(PO_4)_3(OH)$).[146,147]

3.1. Struvite Formation or Crystallization

Struvite is a white, crystalline orthophosphate that consists of magnesium, ammonium, and phosphate in equimolar concentrations (1:1:1), often referred to as MAP (magnesium, ammonium, and phosphate). It is produced under alkaline conditions.[148] It is readily soluble in acid and sparingly soluble in alkaline and neutral conditions.[39] Struvite crystal structure has an orthorhombic unit cell that consists of PO_4^{3-} and NH_4^+ tetrahedral, and $Mg[H_2O]_6^{2+}$ octahedral species.[13] The formation of struvite or struvite crystallization is a phase change technique, where solvated struvite components are converted into a particulate or a precipitate inorganic compound, separated from the liquid solution.[145] It is considered an ideal technique for phosphorus recovery from swine wastewater, anaerobic supernatant, human urine, animal waste slurries, and other waste products.[149] The struvite crystallization technique does not only solve phosphorus-associated wastewater treatment problems, but it also provides an environmentally sustainable, renewable nutrient source for the agriculture sector to be used as a slow-release fertilizer and helps remove nitrogen simultaneously along with phosphate.[23,24,150]

Different types of crystallization reactors have been used for struvite crystallization, such as the mechanically stirred reactor, batch reactor, nonseeded and seeded fluidized bed reactors, water-agitated fluidized bed reactor, air-agitated fluidized bed reactor, gas-agitated fluidized bed reactor, and continuous flow reactor.[151−155] Among these reactors, the nonseeded and seeded fluidized bed reactors are the most commonly used. It has been suggested that seeding reactors offer many advantages, such as optimum crystal size, improved crystal settleability, and enhanced reaction rate.[13,147] In the case of air- and water-agitated reactors, the rapid growth of struvite crystals can reduce the recovery efficiency. Several attempts have been made to optimize the size and improve the separation of the struvite crystals by initiating the precipitation reaction with materials including quartz, silica sands, and periclase grains. Stainless steel, wood, and rubber have also been explored as potential alternatives to traditional seed materials for efficient crystallization processes.[13]

3.2. Struvite Formation Mechanism

Struvite crystallization occurs spontaneously when the combined concentrations of soluble Mg^{2+}, NH_4^+ and PO_4^{3-} either reach or exceed supersaturation level with a pH range of 7 to 11.[148,154] Among the three different saturation regimes (undersaturation, metastable, and supersaturation), the latter is the most desired regime for struvite formation and eventual recovery as a precipitate. Therefore, maintaining the wastewater solutions in a supersaturated phase is necessary and desired for efficient struvite recovery. Supersaturated phases can be achieved by decreasing temperature, increasing concentration, or combining both.[153] It has also been suggested that an increase in pH (7 to 11) increases supersaturation, thus directly influencing struvite crystallization.[22]

Supersaturation primarily controls (i) the induction period before the appearance of the first crystal nuclei (primary nucleation), (ii) the formation of nuclei in the presence of other struvite crystals (secondary nucleation), (iii) crystal growth and the features of crystal interfaces, and thus (iv) the crystal size distribution.[156] Supersaturation (Ω) is calculated using the following expression:

https://doi.org/10.1021/acsenvironau.3c00069
ACS Environ. Au 2024, 4, 271−291

$$\Omega = \frac{a_{Mg^{+2}} \cdot a_{NH_4^+} \cdot a_{PO_4^{3-}}}{K_{sp}}$$

where a is the activity of the ionic species relative to struvite components in solution and K_{sp} is the solubility product of the struvite.

Typically, magnesium is limited in waste streams and is needed to be added in different forms, (i.e., $MgCl_2$, MgO, or $Mg(OH)_2$) to create supersaturation conditions.[145,149] Under such conditions, spontaneous nucleation and crystallization occur rapidly and abundantly without seeding.[13] The general equation for struvite formation is shown below (where $n = 0$, 1 or 2):

$$Mg^{2+} + NH_4^+ + H_nPO_4^{3-n} + 6H_2O \rightarrow MgNH_4PO_4 \cdot 6H_2O + nH^+$$

Similar to other types of crystal formation, the evolution of struvite crystals occurs in two phases: (i) nucleation phase (formation of the seed crystals) and (ii) crystal growth phase (growth of the seed crystals until equilibrium). In the nucleation stage, constituent ions combine to form crystal embryos, called seed crystals. This stage is often divided into primary and secondary nucleation. Primary nucleation is further categorized into homogeneous and heterogeneous nucleation. Homogeneous nucleation is a spontaneous process, in which nucleus formation is not influenced by the presence of other crystals but is rarely observed practically due to the high activation energy required for the formation of a stable seed crystal. On the other hand, heterogeneous processes use system impurities or foreign particles to decrease the activation barrier and, subsequently, increase the crystal nucleation. The nucleation mechanism regarding struvite formation from wastewater is primarily considered a heterogeneous type due to the high impurities or foreign particles found in phosphorus-containing wastewater samples. Here, secondary nucleation occurs in the presence of parent seed crystals via local interactions of existing crystals with reactor walls and impeller.[39,147]

The nucleation process in struvite is often governed by the following equation:[153]

$$J = A \exp\left[\frac{16^3 \nu^2}{k_B{}^3 T^3 (\ln \Omega)^2}\right]$$

where A is the kinetic factor, k_B is the Boltzmann constant, γ is interfacial tension between the crystal and solution, ν is the molecular volume, Ω is the supersaturation ratio, and T is the absolute temperature. The time required for the formation of stable seed crystals is called the induction time. It is affected by various system parameters, including pH, temperature, mixing energy, foreign particle concentration, and supersaturation ratio.

Following successful crystal nucleation, crystal growth involves incorporating constituent ions into the seed crystal lattice to form large, detectable crystals. The crystal growth rate is primarily controlled by the mass transfer mechanisms of constitutive ions and their surface integration. Several theories, including surface energy theory, adsorption layer theory, and diffusion reaction theory, have been proposed to explain the phenomenon of crystal growth. According to the diffusion-reaction theory, once the particles (ions) come in contact with the crystal surface, these particle clusters are eventually diffused toward the seed façade, leading to the evolution of the crystal until a state of equilibrium is reached.[39] Similar to nucleation, the crystal growth process for struvite is also influenced by several parameters, including relative ion (Mg^{2+}, NH_4^+ and PO_4^{3-}) concentrations, initial phases of solutes, presence of competitive ions (Ca^{2+}, Al^{3+}), mixing energy, reaction kinetics and time, pH, thermodynamics of liquid−solid equilibrium, temperature, and degree of supersaturation.[147,157]

3.3. Effect of Solution Parameters on Struvite Crystallization

3.3.1. pH. pH plays an important role in governing the growth rate of the crystallization process, as well as being an indicator of struvite nucleation and its precipitation.[147,158,159] It has been repeatedly reported that the growth rate increases with an increase in pH, with higher growth occurring in the pH range of 8.5 to 9.5.[13,149,151,160,161] The required increase in pH for MAP precipitation can be achieved by adding basic ingredients ($Mg(OH)_2$, $Ca(OH)_2$, NaOH and lime), along with air stripping (stripping of CO_2 by aerating the wastewater stream).[39] It is reported that with a pH increase, the concentration of PO_4^{3-} ions increases while those of Mg^{2+} and NH_4^+ ions decrease, leading to the formation of MAP at pH values >8.5.[145]

Several authors have studied the effect of pH on struvite crystallization. Hao et al. proposed the optimal pH range for struvite (>90%) formation to be 7 to 9 for ultrapure water solutions and 7 to 7.5 for groundwater solutions. These researchers observed that in both solutions, at pH > 9, the white to yellow precipitates were not pure struvite due to the presence of some impurities of $Mg(OH)_2$ and Mg_3PO_4.[162] Ronteltap et al. reported that a pH of 9 or higher is important for the complete formation of struvite from urine.[160] In another study, Wilsenach and co-workers removed 99% of phosphate as struvite from source-separated urine as an MAP precipitatant with the addition of $MgCl_2$ at pH 9.4 and Mg^{2+}:P ratio of 1:1.[149] For KMP (Potassium, magnesium and phosphate) precipitation, only 75% of phosphate was removed at pH 8.2 when Mg:P ratio (Mg^{2+}:P = 2). However, when the pH was further increased from 8.2 to 9 by base addition and modifying the Mg^{2+}:P to 1, the phosphate removal efficiency was increased from 75 to 95% for KMP. Le Corre et al. have shown that pH influences the particle size of struvite crystals due to a negative surface charge present on the crystal surface. With an increase in pH, the zeta potential increases, stabilizing the particles via electrostatic repulsion and leading to smaller crystallites.[163]

3.3.2. Solubility Product. Solubility product is also an important parameter for determining the nucleation, growth, and aggregation kinetics in the precipitation process of struvite.[156] The solubility product constant (K_{sp}) value is defined as the product of the ion activities of each of the constituent ions forming struvite, Mg^{2+}, NH^{4+}, and PO_4^{3-}. Several studies in the literature have reported that the pK_{sp} values range from 9.40 to 13.36.[147] Generally, it is noted that the solubility product decreases with an increase in pH.[22]

3.3.3. Competing Ions. Calcium and magnesium impurities in the solution have been shown to compete with the phosphates, hindering the growth rate of crystalline compounds (struvite) by blocking the active growth sites of the crystal. Zhang et al. investigated the effect of calcium on the struvite crystal shape, size, and purity. It was observed that calcium inhibited crystal growth and led to the formation of an amorphous substance (calcium phosphate) instead of crystalline struvite at a magnesium to calcium molar ratio of 1:1 or above.[150] Other authors have also reported that an increase in

https://doi.org/10.1021/acsenvironau.3c00069
ACS Environ. Au 2024, 4, 271−291

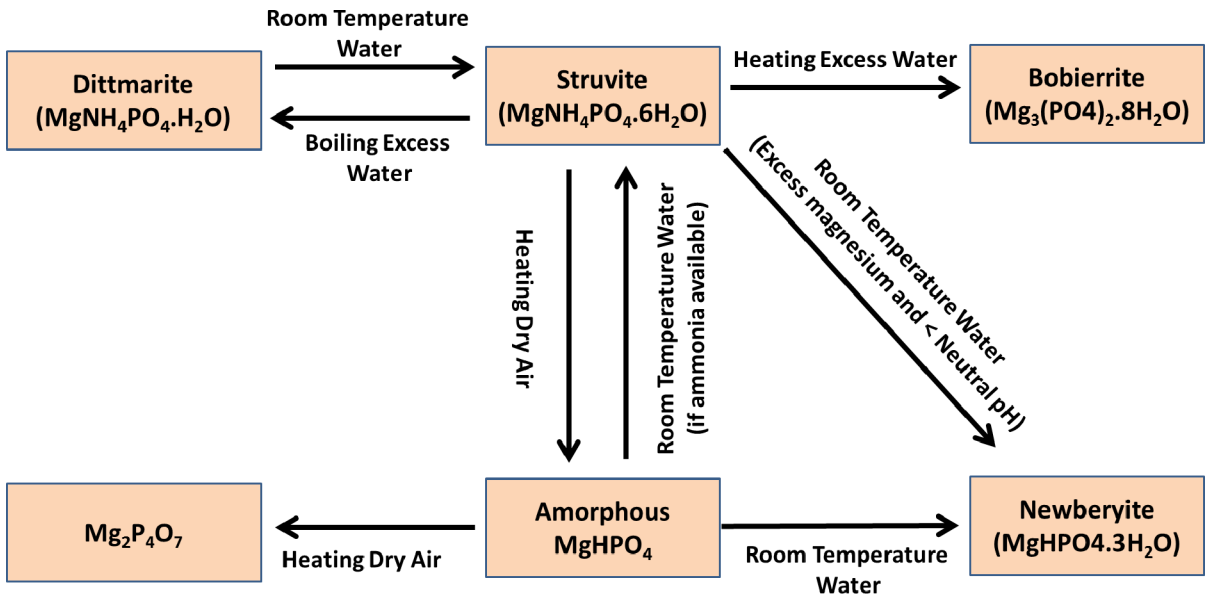

Figure 8. Possible transformation mechanism of various phases associated with struvite. Reproduced with permission from Bhuiyan et al.[165] (Copyright 2008 Elsevier).

calcium concentration inhibits struvite formation.[147,153,162] Due to the high amounts of calcium in sludge liquor, calcium ions interact with the phosphate to form calcium phosphates such as hydroxyapatite or calcium carbonates such as calcite.[153] Hao et al. also evaluated the effect of calcium ions on struvite formation. They found that at a higher pH (pH > 8), more calcium compounds such as Ca_3PO_4 and $CaHPO_4$ were precipitated in the solution and inhibited struvite precipitation.[162] Doyle et al. reported that calcium phosphate apatite precipitation occurred at pH 9.5, whereas effective struvite precipitation occurred at pH 8 and above.[147]

3.3.4. Temperature. Temperature also affects struvite crystallization and influences the solubility product. Struvite formation mainly occurs within a temperature range of 25 to 35 °C. Jones et al. reported that crystallization at low temperatures leads to surface integration-controlled growth, while at high temperatures, it leads to diffusion-controlled growth. These researchers also reported an increase in crystal growth at high temperatures, which influences the morphology of the grown crystals.[164]

3.4. Morphological Characterization of Struvite Crystals

The morphology of struvite crystals has been characterized by several techniques, including XRD, FTIR, SEM, and SEM EDS. Depending on the experimental conditions, struvite crystals have been shown to grow in different high aspect ratio shapes (i.e., coffin-like, rod-like, needle-like, pyramid-like, trapezoidal, dendritic, feather-shaped, and prismatic) and sizes (i.e., dispersed, aggregates, and irregular).

3.5. Transformation of Struvite to Other Forms of Phosphate

Several researchers have investigated the thermal characteristics of struvite and observed the transformation of struvite into other crystalline phases under different temperature conditions. This transformation is associated with the release of ammonia at elevated temperatures, leading to the formation of several different ammonia deficient phases, such as $MgHPO_4{\cdot}3H_2O$ (newberyite), $Mg_3(PO_4)_2{\cdot}8H_2O$ (bobierrite), and $Mg_3(PO_4)_2{\cdot}22H_2O$ (cattiite).[165] Water loss can also lead to water-deficient phases, such as dittmarite ($MgNH_4PO_4{\cdot}H_2O$) and amorphous magnesium hydrogen phosphate. The decomposition of struvite also depends on the nature of the gaseous environment (e.g., nitrogen, partial pressure of water, and humidity).[166]

Bhuiyan et al. investigated the behavior of struvite transformation at various temperatures, as schematically highlighted in Figure 8. These authors synthesized struvite in a pilot-scale fluidized reactor, and found that the struvite decomposition depends upon the heating rate,[165] with the decomposition occurring faster under slow heating conditions. The struvite was transformed into amorphous magnesium hydrogen phosphate by gradually losing ammonia and water, with mass loss beginning at 55 °C and completing when the temperature reached >250 °C). When heated under excess water at a higher temperature (>100 °C), struvite transformed into bobierrite through a gradual ammonia loss. When boiled in excess water, struvite transformed into monohydrate dittmarite by losing its five water molecules. When slowly hydrating dittmarite at room temperature, it was transformed back into the more stable hexahydrate struvite over time.[165]

3.6. Fertilization Aspects of Struvite

Struvite recovered from wastewater contains 52% to 58% phosphate, as compared to 46% in traditional ammonium phosphate fertilizers, and is considered to be the optimal phosphate mineral for slow-release fertilizers. These fertilizers release nutrients at a slower rate, making them suitable for agriculture production operations, potentially substituting traditional phosphate rock fertilizers.[38,154,167,168] It has been shown that more than 90% of dissolved phosphorus can be recovered from anaerobic digester supernatant, and 90 to 100% from urine through struvite crystallization.[24,169−171] The struvite recovered annually from a wastewater treatment plant processing 100 m^3/day would be sufficient to fertilize 2.6 ha of arable land.[24] For fertilization purposes, struvite pellets are suggested to be easily spreadable compared to powder.[172]

The advantages of using struvite include being free of pathogens, having low or no heavy metals, lacking radioactive compounds, being recyclable, having low leaching rates, not burning roots when applied, providing a slow release of nutrients

https://doi.org/10.1021/acsenvironau.3c00069
ACS Environ. Au 2024, 4, 271−291

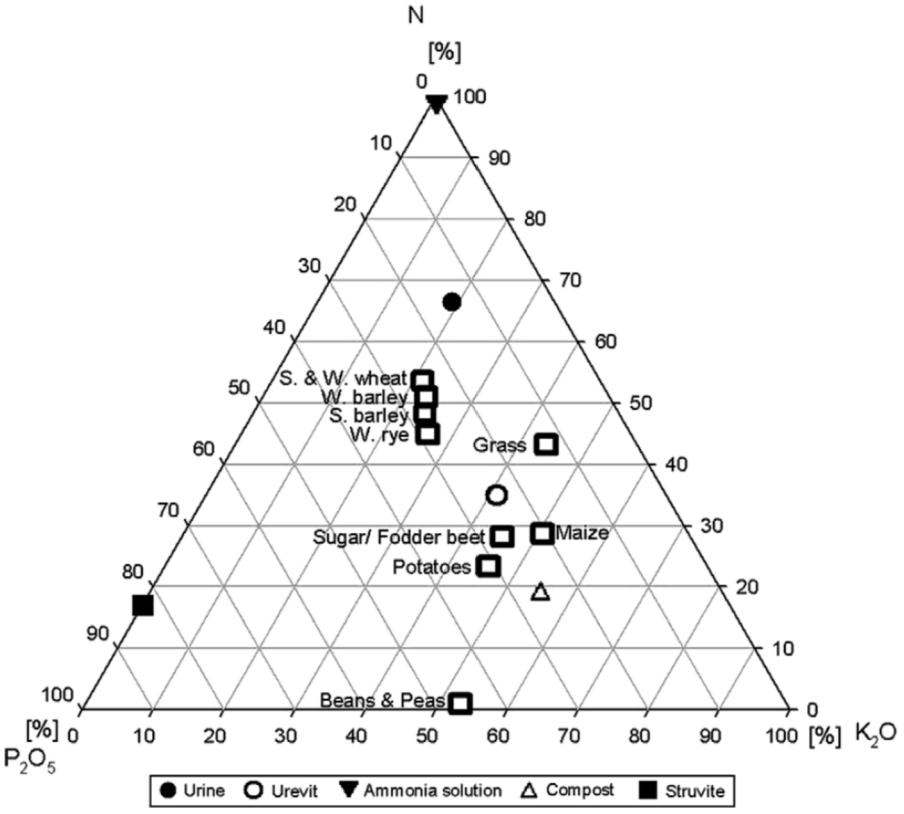

Figure 9. Nutrient compositions in fertilizing products from new sanitation systems and nutrient requirements of common European crops. P (phosphorus) and K (potassium) are represented as P_2O_5 and K_2O to achieve a better visual distribution in the graph. Adapted with permission from Winker et al.[178] (Copyright 2009 Elsevier).

benefiting the plant growth throughout the season, and having lower concentrations of impurities and contaminants compared to other phosphate rock fertilizers (e.g., ammonium phosphate).[24,155,173] Various studies have also found struvite to be as equally effective as water-soluble reference fertilizers in supplying phosphorus to plants, showing improved growth of plants, fruits, various crops, seedlings such as vegetables, turf, ornamentals, orchard trees, forest out-plantings, and potted plants.[167,174]

The slow-release characteristic of struvite fertilizer makes it particularly useful for crops that need Mg^{2+} ions, such as sugar beets.[152] It is also advantageous in coastal agriculture, where it reduces nutrient runoff and the impact of nitrification on coastal waters.[24] In rural areas, phosphorus-containing fertilizers recovered from urine can be directly applied to crops or lawns to enable healthy growth.[175,176]

Gaterell et al. modified struvite with phosphoric acid (denoted as enhanced struvite), which contained two parts of slowly soluble mono hydrogen magnesium phosphate ($MgHPO_4$) to one part of highly soluble diammonium phosphate ($(NH_4)_2HPO_4$). This enhanced struvite is suitable, where high initial doses of phosphate are required followed by a slow release of phosphate.[177] Antonini et al. precipitated six different urine-derived struvite fertilizers and used the fertilizers as phosphorus sources for plants.[167] Greenhouse experiments were performed under local environmental conditions (i.e., light and temperature) on Italian rye grass or maize as test crops in phosphorus-deficient soil. The results showed that phosphorus uptakes of struvite fertilizers by test plants were higher than those induced by a commercial mineral fertilizer. Similarly, Bonvin et al. recovered struvite from various wastewaters. Struvite was applied to ryegrass using synthetic urine-struvite and synthetic nitrified urine fertilizer and was evaluated against 1N1P reference control fertilizer. To calculate the phosphorus uptake via synthetic fertilizers interms of total uptake, the ^{33}P isotope fertilizers were utilized. The authors reported that plants' phosphorus uptake from struvite and nitrified urine fertilizer was 26% of the total uptake, closely matching the 1N1P control fertilizer (28%).[176]

Winker et al. presented important data about nutrients recovered from wastewater to be applied as fertilizers on various crops, as well as crop requirements, as depicted in Figure 9.[178] The figure shows the specific position of each fertilizer within the triangle with nodal points representing pure ammonia solution K_2O and P_2O_5. Here, the struvite is located on the extreme left due to its high phosphate content. It was also suggested fertilizer can be further enhanced efficiently by adding single nutrient mineral fertilizers (if not present in the soil) depending upon the requirement of the crops.[178]

Recently, chemical modeling and response surface methodology combination have been applied to model and optimize conditions for P recovery from aerobic sludge.[179]

3.7. Limitations

Several commercially available struvite crystallization processes are used worldwide including Airprex, Pearl, and PHOSPAQ, and Phosnix.[180] Yet, it is important to note that the bioavailable phosphorus in the resulting struvite recovered from wastewater may not be desirable for direct agricultural application (i.e., commercial fertilizers).[139] A recent technoeconomic assessment was conducted on using struvite crystallization for phosphate recovery from wastewater reported a cost of $6.7−11.2 per kg of

https://doi.org/10.1021/acsenvironau.3c00069
ACS Environ. Au 2024, 4, 271−291

phosphate.[181] Even though the cost can be reduced by scaling up and optimizing the crystallization reactor, researchers have combined struvite crystallization with membrane hybrid systems to optimize the cost. More importantly, cocontaminants (e.g., heavy metals, per-and polyfluoroalkyl substances (PFAS), pathogens, and antimicrobial resistance genes) in wastewater may pose public health and environmental risks. Nakarmi et al. proposed alternative P recovery products, including amorphous Ca−P and Mg−P.[182] Daneshgar et al. conducted a more comprehensive techno-economic and environmental assessment of different phosphate recovery products from aerobic sludge.[183]

4. SUMMARY

As a vital nutrient, phosphorus plays an essential role in the ecosystem. Today, phosphorus is primarily obtained from mined rocks and is often combined in mineral fertilizers with nitrogen, potassium, and sulfuric acid. However, the excessive release of phosphorus from agricultural fertilizer runoff, mining, and industrial activities into water bodies has led to eutrophication. Therefore, phosphate removal and recovery from waste effluents using adsorption, chemical precipitation via crystallization, filtration, urine-source separation methods, and biological methods are considered important environmental steps.

Adsorption, one of the most promising techniques for phosphate removal for several reasons, allows for phosphate removal and recovery for possible reuse. Various adsorbents, including industrial waste, minerals, bioadsorbents, polymers, composites, and magnetic adsorbents, have been explored for phosphate removal. Adsorbate factors, including particle size, specific surface area, surface charge, porosity, and adsorbate structure, affect the adsorbent affinity for phosphate removal. At the same time, experimental parameters (e.g., pH, temperature, and degree of calcination) also play a vital role. While it is challenging to directly compare the adsorption capacities of different adsorbents due to variations in adsorption nature and experimental conditions, specific trends are often observed. It can be concluded that (i) a direct correlation exists between specific surface area and adsorption capacity, (ii) adsorption capacities are higher at lower pH and decrease with an increase in pH, often due to acquiring a negative surface charge, (iii) rate of adsorption is noted to increase with temperature, and (iv) anionic impurities such as SO_4^{2-} and HCO_3^- ions hinder and reduce phosphate adsorption. Although numerous studies focused on adsorbents for phosphate removal, many lack advanced characterization to determine the exact mechanism(s). Moreover, few studies investigate phosphate selectivity and adsorption capacity in complex water matrices, where various constituents (e.g., natural organic matter, anions, cations, pathogens, and suspended solids) are present.

MAP or struvite precipitation is another attractive technique for phosphorus nutrient recovery from waste effluents, human/synthetic urine, and the source-separation method for fertilization because of its slow-release nature. A review of the investigated literature suggests that the formation and morphology (long aspect ratio shapes such as needles, coffins, rods, dendritic, etc.) of struvite crystals are mainly influenced by different experimental parameters, including supersaturation ratio, pH, temperature, mixing energy, and the presence of foreign ions. For example, the optimal pH range for struvite formation is identified to be between 8 and 10. Higher pH gives rise to competing precipitation of calcium compounds and inhibits struvite preparation by blocking active growth sites. Struvite can transform into other water- or ammonia-deficient crystalline phases during thermal treatment under different experimental stimuli (excess water, dry air, etc.). Struvite recovery via the treatment of source-separated urine in decentralized plants has also emerged as an innovation sanitation system aiming at reducing environmental pollution and simplifying nutrient recovery.

AUTHOR INFORMATION

Corresponding Author

Mallikarjuna N. Nadagouda − *Center for Environmental Solutions and Emergency Response, United States Environmental Protection Agency, Cincinnati, Ohio 45268, United States;* orcid.org/0000-0002-4800-4436; Email: nadagouda.mallikarjuna@epa.gov

Authors

Gaiven Varshney − *Department of Engineering Physics, Nuclear Expertise for Advanced Technology (NEAT) Center, Air Force Institute of Technology, Wright-Patterson Air Force Base, Ohio 45433, United States; Center for Environmental Solutions and Emergency Response, United States Environmental Protection Agency, Cincinnati, Ohio 45268, United States*

Vikas Varshney − *Materials and Manufacturing Directorate, Air Force Research Laboratory, Wright-Patterson Air Force Base, Ohio 45433, United States;* orcid.org/0000-0002-2613-458X

Charifa A. Hejase − *Department of Chemical and Environmental Engineering, University of Cincinnati, Cincinnati, Ohio 45221, United States; Pegasus Technical Services INC., Cincinnati, Ohio 45219, United States*

Complete contact information is available at: https://pubs.acs.org/10.1021/acsenvironau.3c00069

Author Contributions

CRediT: **Mallikarjuna N Nadagouda** conceptualization, project administration, resources, supervision, writing-review & editing; **Gaiven Varshney** writing-review & editing; **Vikas Varshney** writing-review & editing; **Charifa A. Hejase** writing-review & editing.

Notes

The U.S. Environmental Protection Agency, through its Office of Research and Development, funded and managed, or partially funded and collaborated in, the research described herein. It has been subjected to the Agency's administrative review and has been approved for external publication. Any opinions expressed in this paper are those of the author(s) and do not necessarily reflect the views of the Agency. Therefore, no official endorsement should be inferred. Any mention of trade names or commercial products does not constitute endorsement or recommendation for use.

The authors declare no competing financial interest.

ABBREVIATIONS

Al-Bent	Hydroxy-aluminum pillared bentonite
ACF-La	Lanthanum doped activated carbon fiber
B33	Bayoxide
B33/Ag	Bayoxide modified with silver
B33/Mn	Bayoxide modified with manganese
Cell-*g*-E/PEI	Amine functionalized epichlorohydrin-grafted cellulose

https://doi.org/10.1021/acsenvironau.3c00069
ACS Environ. Au 2024, 4, 271−291

CMOMO	Composite metal oxides derived from manganese ore tailings
DT-MSMPR	Draft tube mixed suspension mixed product removal crystallizer
EBPR	Enhanced biological phosphorus removal
ESEM	Environmental scanning electron microscope
EDX/EDS	Energy dispersive X-ray spectroscopy
FTIR	Fourier transform infrared spectroscopy
Fe-Bent	Hydroxy-iron pillared bentonite
GPA	Granula palygorskite
GAOs	Glycogen accumulating organisms
HR-SEM	High-resolution scanning electron microscope
HFeO	Fe(III) onto an anion exchange resin
HZrO	Zr(IV) onto an anion exchange resin
HCuO	Cu(III) onto an anion exchange resin
HZO-201	Nanosized hydrous zirconium oxide supported by anion exchanger D-201
ICP-AES	Inductively coupled plasma atomic emission spectrometry
KMP	Potassium, magnesium and phosphate
LDHs	Layered double hydroxides
LSCC	La(III)-loaded silica-chitosan composite
LCB	La(III)-loaded cross-linked chitosan beads
LDR	La(III)-loaded Duolite C 466
LO	Lanthanum oxide
MTZ	Mass transfer zone
MAP	Magnesium, ammonium and phosphate
MF-FOMBR	Hybrid microfiltration-forward osmosis membrane bioreactor
MPP	Phosphate and potassium struvite
Mg:K:P	Magnesium, potassium and phosphorus ratios
PD	Pore diameter
PV	Pore volume
PAOs	Phosphorus accumulating organisms
SEM	Scanning electron microscopy
TEM	Transmission electron microscopy
TDPA-KCl	Thermal decomposition product of alunite and potassium chloride mixture
XPS	X-ray photoelectron spectroscopy
XRD	X-ray diffraction analysis

REFERENCES

(1) Su, Y.; Cui, H.; Li, Q.; Gao, S.; Shang, J. K. Strong adsorption of phosphate by amorphous zirconium oxide nanoparticles. *Water research* **2013**, *47* (14), 5018.

(2) Jing, L.; Qin, X.; Luan, Y.; Qu, Y.; Xie, M. Synthesis of efficient TiO2-based photocatalysts by phosphate surface modification and the activity-enhanced mechanisms. *Appl. Surf. Sci.* **2012**, *258* (8), 3340.

(3) Roguska, A.; Hiromoto, S.; Yamamoto, A.; Woźniak, M. J.; Pisarek, M.; Lewandowska, M. Collagen immobilization on 316L stainless steel surface with cathodic deposition of calcium phosphate. *Appl. Surf. Sci.* **2011**, *257* (11), 5037.

(4) Lusquiños, F.; Pou, J.; Boutinguiza, M.; Quintero, F.; Soto, R.; León, B.; Pérez-Amor, M. Main characteristics of calcium phosphate coatings obtained by laser cladding. *Appl. Surf. Sci.* **2005**, *247* (1−4), 486.

(5) Nadagouda, M. N.; Schock, M.; Metz, D. H.; DeSantis, M. K.; Lytle, D.; Welch, M. Effect of phosphate inhibitors on the formation of lead phosphate/carbonate nanorods, microrods, and dendritic structures. *Cryst. Growth Des.* **2009**, *9* (4), 1798.

(6) Li, G.; Gao, S.; Zhang, G.; Zhang, X. Enhanced adsorption of phosphate from aqueous solution by nanostructured iron (III)-copper (II) binary oxides. *Chemical Engineering Journal* **2014**, *235*, 124.

(7) Deng, L.; Shi, Z. Synthesis and characterization of a novel Mg-Al hydrotalcite-loaded kaolin clay and its adsorption properties for phosphate in aqueous solution. *J. Alloys Compd.* **2015**, *637*, 188.

(8) Song, X.; Pan, Y.; Wu, Q.; Cheng, Z.; Ma, W. Phosphate removal from aqueous solutions by adsorption using ferric sludge. *Desalination* **2011**, *280* (1−3), 384.

(9) Huang, W.; Chen, J.; He, F.; Tang, J.; Li, D.; Zhu, Y.; Zhang, Y. Effective phosphate adsorption by Zr/Al-pillared montmorillonite: insight into equilibrium, kinetics and thermodynamics. *Appl. Clay Sci.* **2015**, *104*, 252.

(10) Huang, W.-Y.; Zhu, R.-H.; He, F.; Li, D.; Zhu, Y.; Zhang, Y.-M. Enhanced phosphate removal from aqueous solution by ferric-modified laterites: Equilibrium, kinetics and thermodynamic studies. *Chemical engineering journal* **2013**, *228*, 679.

(11) Liu, X.; Zhang, L. Removal of phosphate anions using the modified chitosan beads: adsorption kinetic, isotherm and mechanism studies. *Powder Technol.* **2015**, *277*, 112.

(12) Yu, Q.; Zheng, Y.; Wang, Y.; Shen, L.; Wang, H.; Zheng, Y.; He, N.; Li, Q. Highly selective adsorption of phosphate by pyromellitic acid intercalated ZnAl-LDHs: assembling hydrogen bond acceptor sites. *Chemical Engineering Journal* **2015**, *260*, 809.

(13) Ye, Z.; Shen, Y.; Ye, X.; Zhang, Z.; Chen, S.; Shi, J. Phosphorus recovery from wastewater by struvite crystallization: Property of aggregates. *Journal of Environmental Sciences* **2014**, *26* (5), 991.

(14) Mihelcic, J. R.; Fry, L. M.; Shaw, R. Global potential of phosphorus recovery from human urine and feces. *Chemosphere* **2011**, *84* (6), 832.

(15) Yu, Y.; Chen, J. P. Key factors for optimum performance in phosphate removal from contaminated water by a Fe-Mg-La tri-metal composite sorbent. *J. Colloid Interface Sci.* **2015**, *445*, 303.

(16) Peleka, E. N.; Deliyanni, E. A. Adsorptive removal of phosphates from aqueous solutions. *Desalination* **2009**, *245* (1−3), 357.

(17) Cooper, J.; Lombardi, R.; Boardman, D.; Carliell-Marquet, C. The future distribution and production of global phosphate rock reserves. *Resources, Conservation and Recycling* **2011**, *57*, 78.

(18) Van Vuuren, D. P.; Bouwman, A. F.; Beusen, A. H. Phosphorus demand for the 1970−2100 period: a scenario analysis of resource depletion. *Global environmental change* **2010**, *20* (3), 428.

(19) Cordell, D.; Drangert, J.-O.; White, S. The story of phosphorus: Global food security and food for thought. *Global Environmental Change* **2009**, *19* (2), 292.

(20) Brinck, J. W. In *Ciba Foundation Symposium 57 - Phosphorus in the Enviroment: Its Chemistry and Biochemistry*; John Wiley & Sons, Ltd., 2008; Vol. *57*.

(21) Stewart, W. M.; Hammond, L. L.; Van Kauwenbergh, S. J.; Sims, J.; Sharpley, A.Phosphorus as a natural resource. *Phosphorus: agriculture and the environment*; American Society of Agronomy, Inc., 2005; Vol. *46*, p 3.

(22) Kozik, A.; Hutnik, N.; Piotrowski, K.; Matynia, A. Continuous reaction crystallization of struvite from diluted aqueous solution of phosphate(V) ions in the presence of magnesium ions excess. *Chem. Eng. Res. Des.* **2014**, *92* (3), 481.

(23) Wang, C. C.; Hao, X. D.; Guo, G. S.; van Loosdrecht, M. C. M. Formation of pure struvite at neutral pH by electrochemical deposition. *Chemical Engineering Journal* **2010**, *159* (1−3), 280.

(24) Shu, L.; Schneider, P.; Jegatheesan, V.; Johnson, J. An economic evaluation of phosphorus recovery as struvite from digester supernatant. *Bioresource technology* **2006**, *97* (17), 2211.

(25) Nguyen, T. A.; Ngo, H. H.; Guo, W. S.; Zhang, J.; Liang, S.; Lee, D. J.; Nguyen, P. D.; Bui, X. T. Modification of agricultural waste/by-products for enhanced phosphate removal and recovery: potential and obstacles. *Bioresour. Technol.* **2014**, *169*, 750.

(26) Liu, J.; Wan, L.; Zhang, L.; Zhou, Q. Effect of pH, ionic strength, and temperature on the phosphate adsorption onto lanthanum-doped activated carbon fiber. *J. Colloid Interface Sci.* **2011**, *364* (2), 490.

(27) Arshadi, M.; Foroughifard, S.; Etemad Gholtash, J.; Abbaspourrad, A. Preparation of iron nanoparticles-loaded Spondias purpurea seed waste as an excellent adsorbent for removal of phosphate from synthetic and natural waters. *J. Colloid Interface Sci.* **2015**, *452*, 69.

https://doi.org/10.1021/acsenvironau.3c00069
ACS Environ. Au 2024, 4, 271−291

(28) Babatunde, A. O.; Zhao, Y. Q. Equilibrium and kinetic analysis of phosphorus adsorption from aqueous solution using waste alum sludge. *Journal of Hazardous Materials* **2010**, *184* (1−3), 746.
(29) Huang, W.-Y.; Li, D.; Liu, Z.-Q.; Tao, Q.; Zhu, Y.; Yang, J.; Zhang, Y.-M. Kinetics, isotherm, thermodynamic, and adsorption mechanism studies of La(OH)3-modified exfoliated vermiculites as highly efficient phosphate adsorbents. *Chemical Engineering Journal* **2014**, *236*, 191.
(30) Yu, Y.; Wu, R.; Clark, M. Phosphate removal by hydrothermally modified fumed silica and pulverized oyster shell. *J. Colloid Interface Sci.* **2010**, *350* (2), 538.
(31) Jia, C.; Dai, Y.; Wu, C.; Wu, Z. B.; Liang, W. Adsorption charecterstics of used cement for phosphorous removal from wastewater. *Fresenius Environ. Bull.* **2013**, *22* (10), 2910.
(32) Xie, J.; Lin, Y.; Li, C.; Wu, D.; Kong, H. Removal and recovery of phosphate from water by activated aluminum oxide and lanthanum oxide. *Powder Technol.* **2015**, *269*, 351.
(33) Wu, B.; Wan, J.; Zhang, Y.; Pan, B.; Lo, I. M. Selective phosphate removal from water and wastewater using sorption: process fundamentals and removal mechanisms. *Environ. Sci. Technol.* **2020**, *54* (1), 50.
(34) Bacelo, H.; Pintor, A. M.; Santos, S. C.; Boaventura, R. A.; Botelho, C. M. Performance and prospects of different adsorbents for phosphorus uptake and recovery from water. *Chemical Engineering Journal* **2020**, *381*, 122566.
(35) Hube, S.; Eskafi, M.; Hrafnkelsdóttir, K. F.; Bjarnadóttir, B.; Bjarnadóttir, M. Á.; Axelsdóttir, S.; Wu, B. Direct membrane filtration for wastewater treatment and resource recovery: A review. *Science of the total environment* **2020**, *710*, 136375.
(36) Novillo, C.; Guaya, D.; Allen-Perkins Avendaño, A.; Armijos, C.; Cortina, J. L.; Cota, I. Evaluation of phosphate removal capacity of Mg/Al layered double hydroxides from aqueous solutions. *Fuel* **2014**, *138*, 72.
(37) Vohla, C.; Kõiv, M.; Bavor, H. J.; Chazarenc, F.; Mander, D. C. Filter materials for phosphorus removal from wastewater in treatment wetlands—A review. *Ecological Engineering* **2011**, *37* (1), 70.
(38) Hao, X.; Wang, C.; van Loosdrecht, M. C.; Hu, Y. Looking beyond struvite for P-recovery. *Environ. Sci. Technol.* **2013**, *47* (10), 4965.
(39) Liu, Y.; Kumar, S.; Kwag, J.-H.; Ra, C. Magnesium ammonium phosphate formation, recovery and its application as valuable resources: a review. *J. Chem. Technol. Biotechnol.* **2013**, *88* (2), 181.
(40) Liu, J.; Zhou, Q.; Chen, J.; Zhang, L.; Chang, N. Phosphate adsorption on hydroxyl-iron-lanthanum doped activated carbon fiber. *Chemical Engineering Journal* **2013**, *215−216*, 859.
(41) Ren, J.; Li, N.; Zhao, L.; Ren, N. Enhanced adsorption of phosphate by loading nanosized ferric oxyhydroxide on anion resin. *Frontiers of Environmental Science & Engineering* **2014**, *8* (4), 531.
(42) Zeng, L.; Li, X.; Liu, J. Adsorptive removal of phosphate from aqueous solutions using iron oxide tailings. *Water Res.* **2004**, *38* (5), 1318.
(43) Zamparas, M.; Gavriil, G.; Coutelieris, F. A.; Zacharias, I. A theoretical and experimental study on the P-adsorption capacity of Phoslock. *Appl. Surf. Sci.* **2015**, *335*, 147.
(44) Yadav, D.; Kapur, M.; Kumar, P.; Mondal, M. K. Adsorptive removal of phosphate from aqueous solution using rice husk and fruit juice residue. *Process Safety and Environmental Protection* **2015**, *94*, 402.
(45) Xie, J.; Wang, Z.; Lu, S.; Wu, D.; Zhang, Z.; Kong, H. Removal and recovery of phosphate from water by lanthanum hydroxide materials. *Chemical Engineering Journal* **2014**, *254*, 163.
(46) Choi, J.-W.; Lee, S.-Y.; Lee, S.-H.; Kim, J.-E.; Park, K.-Y.; Kim, D.-J.; Hong, S.-W. Comparison of Surface-Modified Adsorbents for Phosphate Removal in Water. *Water, Air, & Soil Pollution* **2012**, *223* (6), 2881.
(47) Yin, H.; Kong, M. Simultaneous removal of ammonium and phosphate from eutrophic waters using natural calcium-rich attapulgite-based versatile adsorbent. *Desalination* **2014**, *351*, 128.
(48) Xue, Y.; Hou, H.; Zhu, S. Characteristics and mechanisms of phosphate adsorption onto basic oxygen furnace slag. *Journal of Hazardous Materials* **2009**, *162* (2−3), 973.
(49) Lalley, J.; Han, C.; Li, X.; Dionysiou, D. D.; Nadagouda, M. N. Phosphate adsorption using modified iron oxide-based sorbents in lake water: Kinetics, equilibrium, and column tests. *Chemical Engineering Journal* **2016**, *284*, 1386.
(50) Abou Taleb, M. F.; Mahmoud, G. A.; Elsigeny, S. M.; Hegazy, E.-S. A. Adsorption and desorption of phosphate and nitrate ions using quaternary (polypropylene-g-N,N-dimethylamino ethylmethacrylate) graft copolymer. *Journal of Hazardous Materials* **2008**, *159* (2−3), 372.
(51) Akar, S. T.; Tosun, I.; Ozcan, A.; Gedikbey, T. Phosphate removal potential of the adsorbent material prepared from thermal decomposition of alunite ore-KCl mixture in environmental cleanup. *Desalination* **2010**, *260* (1−3), 107.
(52) Cheng, X.; Huang, X.; Wang, X.; Zhao, B.; Chen, A.; Sun, D. Phosphate adsorption from sewage sludge filtrate using zinc-aluminum layered double hydroxides. *Journal of Hazardous Materials* **2009**, *169* (1−3), 958.
(53) Xiong, J. B.; Mahmood, Q. Adsorptive removal of phosphate from aqueous media by peat. *Desalination* **2010**, *259* (1−3), 59.
(54) Park, J.-H.; Wang, J. J.; Xiao, R.; Zhou, B.; Delaune, R. D.; Seo, D.-C. Effect of pyrolysis temperature on phosphate adsorption characteristics and mechanisms of crawfish char. *J. Colloid Interface Sci.* **2018**, *525*, 143.
(55) Martin, E.; Lalley, J.; Wang, W.; Nadagouda, M. N.; Sahle-Demessie, E.; Chae, S.-R. Phosphate recovery from water using cellulose enhanced magnesium carbonate pellets: Kinetics, isotherms, and desorption. *Chemical Engineering Journal* **2018**, *352*, 612.
(56) Liu, C.-j.; Li, Y.-z.; Luan, Z.-k.; Chen, Z.-y.; Zhang, Z.-g.; Jia, Z.-p. Adsorption removal of phosphate from aqueous solution by active red mud. *Journal of Environmental Sciences* **2007**, *19* (10), 1166.
(57) Han, C.; Lalley, J.; Iyanna, N.; Nadagouda, M. N. Removal of phosphate using calcium and magnesium-modified iron-based adsorbents. *Mater. Chem. Phys.* **2017**, *198*, 115.
(58) Nakarmi, A.; Bourdo, S. E.; Ruhl, L.; Kanel, S.; Nadagouda, M.; Alla, P. K.; Pavel, I.; Viswanathan, T. Benign zinc oxide betaine-modified biochar nanocomposites for phosphate removal from aqueous solutions. *Journal of environmental management* **2020**, *272*, 111048.
(59) Yang, W.; Shi, X.; Dong, H.; Tang, H.; Chen, W.; Wu, M.; Hua, M.; Zhang, W. Fabrication of a reusable polymer-based cerium hydroxide nanocomposite with high stability for preferable phosphate removal. *Chemical Engineering Journal* **2021**, *405*, 126649.
(60) Huo, J.; Min, X.; Wang, Y. Zirconium-modified natural clays for phosphate removal: Effect of clay minerals. *Environmental Research* **2021**, *194*, 110685.
(61) Jutidamrongphan, W.; Park, K. Y.; Dockko, S.; Choi, J. W.; Lee, S. H. High removal of phosphate from wastewater using silica sulfate. *Environ. Chem. Lett.* **2012**, *10* (1), 21.
(62) Gao, Z.; Wei, Y.; Tian, X.; Liu, Y.; Lan, X.; Zhang, D.; Han, S.; Huo, P. A novel Ce/Fe bimetallic metal-organic framework with ortho-dodecahedral multilevel structure for enhanced phosphate adsorption. *Chemical Engineering Journal* **2024**, *486*, 150284.
(63) Li, G.; Chen, D.; Zhao, W.; Zhang, X. Efficient adsorption behavior of phosphate on La-modified tourmaline. *Journal of Environmental Chemical Engineering* **2015**, *3* (1), 515.
(64) Eltaweil, A. S.; Ibrahim, K.; Abd El-Monaem, E. M.; El-Subruiti, G. M.; Omer, A. M. Phosphate removal by Lanthanum-doped aminated graphene oxide@ aminated chitosan microspheres: Insights into the adsorption mechanism. *Journal of Cleaner Production* **2023**, *385*, 135640.
(65) Ren, Z.; Shao, L.; Zhang, G. Adsorption of Phosphate from Aqueous Solution Using an Iron-Zirconium Binary Oxide Sorbent. *Water, Air, & Soil Pollution* **2012**, *223* (7), 4221.
(66) Zhang, G.; Liu, H.; Liu, R.; Qu, J. Removal of phosphate from water by a Fe-Mn binary oxide adsorbent. *J. Colloid Interface Sci.* **2009**, *335* (2), 168.
(67) Su, Y.; Yang, W.; Sun, W.; Li, Q.; Shang, J. K. Synthesis of mesoporous cerium-zirconium binary oxide nanoadsorbents by a

solvothermal process and their effective adsorption of phosphate from water. *Chemical Engineering Journal* **2015**, *268*, 270.
(68) Lu, J.; Liu, D.; Hao, J.; Zhang, G.; Lu, B. Phosphate removal from aqueous solutions by a nano-structured Fe-Ti bimetal oxide sorbent. *Chem. Eng. Res. Des.* **2015**, *93*, 652.
(69) Lalley, J.; Han, C.; Mohan, G. R.; Dionysiou, D. D.; Speth, T. F.; Garland, J.; Nadagouda, M. N. Phosphate removal using modified Bayoxide® E33 adsorption media. *Environmental Science: Water Research & Technology* **2015**, *1* (1), 96.
(70) Liang, H.; Liu, J.; Wei, Y.; Guo, X. Evaluation of phosphorus removal from wastewater by soils in rural areas in China. *Journal of Environmental Sciences* **2010**, *22* (1), 15.
(71) Du, M.; Zhang, Y.; Wang, Z.; Lv, M.; Tang, A.; Yu, Y.; Qu, X.; Chen, Z.; Wen, Q.; Li, A. Insight into the synthesis and adsorption mechanism of adsorbents for efficient phosphate removal: Exploration from synthesis to modification. *Chemical Engineering Journal* **2022**, *442*, 136147.
(72) Eljamal, O.; Okawauchi, J.; Hiramatsu, K.; Harada, M. Phosphorus sorption from aqueous solution using natural materials. *Environmental earth sciences* **2013**, *68*, 859.
(73) Grace, M. A.; Healy, M. G.; Clifford, E. Use of industrial by-products and natural media to adsorb nutrients, metals and organic carbon from drinking water. *Science of the total environment* **2015**, *518*−*519*, 491.
(74) Guaya, D.; Valderrama, C.; Farran, A.; Armijos, C.; Cortina, J. L. Simultaneous phosphate and ammonium removal from aqueous solution by a hydrated aluminum oxide modified natural zeolite. *Chemical Engineering Journal* **2015**, *271*, 204.
(75) Johnston, A. E.; Richards, I. R. Effectiveness of different precipitated phosphates as phosphorus sources for plants. *Soil Use and Management* **2003**, *19* (1), 45.
(76) Fan, T.; Wang, M.; Wang, X.; Chen, Y.; Wang, S.; Zhan, H.; Chen, X.; Lu, A.; Zha, S. Experimental study of the adsorption of nitrogen and phosphorus by natural clay minerals. *Adsorption Science & Technology* **2021**, *2021*, 1.
(77) Yan, L. G.; Xu, Y. Y.; Yu, H. Q.; Xin, X. D.; Wei, Q.; Du, B. Adsorption of phosphate from aqueous solution by hydroxy-aluminum, hydroxy-iron and hydroxy-iron-aluminum pillared bentonites. *Journal of Hazardous Materials* **2010**, *179* (1−3), 244.
(78) Perassi, I.; Borgnino, L. Adsorption and surface precipitation of phosphate onto CaCO3-montmorillonite: effect of pH, ionic strength and competition with humic acid. *Geoderma* **2014**, *232*−*234*, 600.
(79) Kumar, E.; Bhatnagar, A.; Hogland, W.; Marques, M.; Sillanpaa, M. Interaction of anionic pollutants with Al-based adsorbents in aqueous media - A review. *Chemical Engineering Journal* **2014**, *241*, 443.
(80) Yin, H.; Kong, M.; Fan, C. Batch investigations on P immobilization from wastewaters and sediment using natural calcium rich sepiolite as a reactive material. *Water Res.* **2013**, *47* (13), 4247.
(81) Yan, L. G.; Yang, K.; Shan, R. R.; Yan, T.; Wei, J.; Yu, S. J.; Yu, H. Q.; Du, B. Kinetic, isotherm and thermodynamic investigations of phosphate adsorption onto core-shell Fe(3)O(4)@LDHs composites with easy magnetic separation assistance. *J. Colloid Interface Sci.* **2015**, *448*, 508.
(82) Wang, Y.; Sun, D. Phosphate removal from aqueous solutions on fly ash with medium calcium content. *Korean Journal of Chemical Engineering* **2015**, *32* (7), 1323.
(83) Li, Y.; Liu, C.; Luan, Z.; Peng, X.; Zhu, C.; Chen, Z.; Zhang, Z.; Fan, J.; Jia, Z. Phosphate removal from aqueous solutions using raw and activated red mud and fly ash. *Journal of Hazardous Materials* **2006**, *B137* (1), 374.
(84) Lu, S. G.; Bai, S. Q.; Zhu, L.; Shan, H. D. Removal mechanism of phosphate from aqueous solution by fly ash. *Journal of Hazardous Materials* **2009**, *161* (1), 95.
(85) Hashim, K. S.; Ewadh, H. M.; Muhsin, A. A.; Zubaidi, S. L.; Kot, P.; Muradov, M.; Aljefery, M.; Al-Khaddar, R. Phosphate removal from water using bottom ash: Adsorption performance, coexisting anions and modelling studies. *Water Sci. Technol.* **2021**, *83* (1), 77.
(86) Zhao, Y.; Yue, Q.; Li, Q.; Xu, X.; Yang, Z.; Wang, X.; Gao, B.; Yu, H. Characterization of red mud granular adsorbent (RMGA) and its performance on phosphate removal from aqueous solution. *Chemical Engineering Journal* **2012**, *193*−*194*, 161.
(87) Yu, J.; Liang, W.; Wang, L.; Li, F.; Zou, Y.; Wang, H. Phosphate removal from domestic wastewater using thermally modified steel slag. *Journal of Environmental Sciences* **2015**, *31*, 81.
(88) Yang, Y.; Zhao, Y.; Babatunde, A.; Wang, L.; Ren, Y.; Han, Y. Characteristics and mechanisms of phosphate adsorption on dewatered alum sludge. *Sep. Purif. Technol.* **2006**, *51* (2), 193.
(89) Huang, X.; Liao, X.; Shi, B. Adsorption removal of phosphate in industrial wastewater by using metal-loaded skin split waste. *Journal of Hazardous Materials* **2009**, *166* (2−3), 1261.
(90) Iizuka, A.; Sasaki, T.; Hongo, T.; Honma, M.; Hayakawa, Y.; Yamasaki, A.; Yanagisawa, Y. Phosphorus Adsorbent Derived from Concrete Sludge (PAdeCS) and its Phosphorus Recovery Performance. *Ind. Eng. Chem. Res.* **2012**, *51* (34), 11266.
(91) Long, F.; Gong, J.-L.; Zeng, G.-M.; Chen, L.; Wang, X.-Y.; Deng, J.-H.; Niu, Q.-Y.; Zhang, H.-Y.; Zhang, X.-R. Removal of phosphate from aqueous solution by magnetic Fe-Zr binary oxide. *Chemical Engineering Journal* **2011**, *171* (2), 448.
(92) Antelo, J.; Arce, F.; Fiol, S. Arsenate and phosphate adsorption on ferrihydrite nanoparticles. Synergetic interaction with calcium ions. *Chem. Geol.* **2015**, *410*, 53.
(93) Sowmya, A.; Meenakshi, S. Phosphate uptake studies on different types of lanthanum-loaded polymeric materials. *Environmental Progress & Sustainable Energy* **2015**, *34* (1), 146.
(94) Fierro, S.; Sanchez-Saavedra Mdel, P.; Copalcua, C. Nitrate and phosphate removal by chitosan immobilized Scenedesmus. *Bioresource technology* **2008**, *99* (5), 1274.
(95) Chiou, C.-S.; Lin, Y.-F.; Chen, H.-W.; Chang, C.-C.; Chang, S.-H. Adsorption of Phosphate in Aqueous Solution by Magnetite Modified with Diethylenetriamine. *J. Nanosci. Nanotechnol.* **2015**, *15* (4), 2850.
(96) Wang, W.; Zhang, H.; Zhang, L.; Wan, H.; Zheng, S.; Xu, Z. Adsorptive removal of phosphate by magnetic Fe3O4@C@ZrO2. *Colloids Surf., A* **2015**, *469*, 100.
(97) Almanassra, I. W.; Kochkodan, V.; Mckay, G.; Atieh, M. A.; Al-Ansari, T. Review of phosphate removal from water by carbonaceous sorbents. *Journal of environmental management* **2021**, *287*, 112245.
(98) Qiu, H.; Lv, L.; Pan, B.-c.; Zhang, Q.-j.; Zhang, W.-m.; Zhang, Q.-x. Critical review in adsorption kinetic models. *Journal of Zhejiang University SCIENCE A* **2009**, *10* (5), 716.
(99) Zhang, L.; Zhou, Q.; Liu, J.; Chang, N.; Wan, L.; Chen, J. Phosphate adsorption on lanthanum hydroxide-doped activated carbon fiber. *Chemical Engineering Journal* **2012**, *185*−*186*, 160.
(100) Zhou, Q.; Wang, X.; Liu, J.; Zhang, L. Phosphorus removal from wastewater using nano-particulates of hydrated ferric oxide doped activated carbon fiber prepared by Sol-Gel method. *Chemical Engineering Journal* **2012**, *200*−*202*, 619.
(101) Verma, S.; Nadagouda, M. N. Graphene-based composites for phosphate removal. *ACS omega* **2021**, *6* (6), 4119.
(102) Almanassra, I. W.; Mckay, G.; Kochkodan, V.; Atieh, M. A.; Al-Ansari, T. A state of the art review on phosphate removal from water by biochars. *Chemical Engineering Journal* **2021**, *409*, 128211.
(103) Zhang, M.; Song, G.; Gelardi, D. L.; Huang, L.; Khan, E.; Mašek, O.; Parikh, S. J.; Ok, Y. S. Evaluating biochar and its modifications for the removal of ammonium, nitrate, and phosphate in water. *Water Res.* **2020**, *186*, 116303.
(104) Zhu, Z.; Zeng, H.; Zhu, Y.; Yang, F.; Zhu, H.; Qin, H.; Wei, W. Kinetics and thermodynamic study of phosphate adsorption on the porous biomorph-genetic composite of α-Fe2O3/Fe3O4/C with eucalyptus wood microstructure. *Sep. Purif. Technol.* **2013**, *117*, 124.
(105) Nguyen, T. A.; Ngo, H. H.; Guo, W. S.; Pham, T. Q.; Li, F. M.; Nguyen, T. V.; Bui, X. T. Adsorption of phosphate from aqueous solutions and sewage using zirconium loaded okara (ZLO): Fixed-bed column study. *Science of the total environment* **2015**, *523*, 40.
(106) Eberhardt, T. L.; Min, S. H. Biosorbents prepared from wood particles treated with anionic polymer and iron salt: effect of particle size on phosphate adsorption. *Bioresource technology* **2008**, *99* (3), 626.

https://doi.org/10.1021/acsenvironau.3c00069
ACS Environ. Au 2024, 4, 271−291

(107) Xu, X.; Gao, B.; Wang, W.; Yue, Q.; Wang, Y.; Ni, S. Adsorption of phosphate from aqueous solutions onto modified wheat residue: characteristics, kinetic and column studies. *Colloids and surfaces. B, Biointerfaces* **2009**, *70* (1), 46.
(108) Mangwandi, C.; Albadarin, A. B.; Glocheux, Y.; Walker, G. M. Removal of ortho-phosphate from aqueous solution by adsorption onto dolomite. *Journal of Environmental Chemical Engineering* **2014**, *2* (2), 1123.
(109) Wang, H.; Zhu, J.; Fu, Q.-L.; Xiong, J.-W.; Hong, C.; Hu, H.-Q.; Violante, A. Adsorption of Phosphate onto Ferrihydrite and Ferrihydrite-Humic Acid Complexes. *Pedosphere* **2015**, *25* (3), 405.
(110) Jiang, C.; Jia, L.; He, Y.; Zhang, B.; Kirumba, G.; Xie, J. Adsorptive removal of phosphorus from aqueous solution using sponge iron and zeolite. *J. Colloid Interface Sci.* **2013**, *402*, 246.
(111) Chen, L.; Zhao, X.; Pan, B.; Zhang, W.; Hua, M.; Lv, L.; Zhang, W. Preferable removal of phosphate from water using hydrous zirconium oxide-based nanocomposite of high stability. *Journal of Hazardous Materials* **2015**, *284*, 35.
(112) Acelas, N. Y.; Martin, B. D.; Lopez, D.; Jefferson, B. Selective removal of phosphate from wastewater using hydrated metal oxides dispersed within anionic exchange media. *Chemosphere* **2015**, *119*, 1353.
(113) Hua, M.; Xiao, L.; Pan, B.; Zhang, Q. Validation of polymer-based nano-iron oxide in further phosphorus removal from bioeffluent: laboratory and scaledup study. *Frontiers of Environmental Science & Engineering* **2013**, *7* (3), 435.
(114) Loganathan, P.; Vigneswaran, S.; Kandasamy, J.; Bolan, N. S. Removal and Recovery of Phosphate From Water Using Sorption. *Critical Reviews in Environmental Science and Technology* **2014**, *44* (8), 847.
(115) Delaney, P.; McManamon, C.; Hanrahan, J. P.; Copley, M. P.; Holmes, J. D.; Morris, M. A. Development of chemically engineered porous metal oxides for phosphate removal. *Journal of Hazardous Materials* **2011**, *185* (1), 382.
(116) Li, G.; Gao, S.; Zhang, G.; Zhang, X. Enhanced adsorption of phosphate from aqueous solution by nanostructured iron(III)-copper(II) binary oxides. *Chem. Eng. J.* **2014**, *235*, 124.
(117) Anirudhan, T.; Rauf, T. A.; Rejeena, S. Removal and recovery of phosphate ions from aqueous solutions by amine functionalized epichlorohydrin-grafted cellulose. *Desalination* **2012**, *285*, 277.
(118) Liu, T.; Wu, K.; Zeng, L. Removal of phosphorus by a composite metal oxide adsorbent derived from manganese ore tailings. *Journal of Hazardous Materials* **2012**, *217*−*218*, 29.
(119) Eskandarpour, A.; Sassa, K.; Bando, Y.; Okido, M.; Asai, S. Magnetic Removal of Phosphate from Wastewater Using Schwertmannite. *Materials Transactions* **2006**, *47* (7), 1832.
(120) Xue, Y.; Hou, H.; Zhu, S. Characteristics and mechanisms of phosphate adsorption onto basic oxygen furnace slag. *J. Hazard. Mater.* **2009**, *162* (2−3), 973.
(121) Gao, S.; Wang, C.; Pei, Y. Comparison of different phosphate species adsorption by ferric and alum water treatment residuals. *Journal of Environmental Sciences* **2013**, *25* (5), 986.
(122) Shanableh, A. M.; Elsergany, M. M. Removal of phosphate from water using six Al-, Fe-, and Al-Fe-modified bentonite adsorbents. *Journal of Environmental Science and Health, Part A: Environmental Science and Engineering* **2013**, *48* (2), 223.
(123) Yan, Y.; Sun, X.; Ma, F.; Li, J.; Shen, J.; Han, W.; Liu, X.; Wang, L. Removal of phosphate from etching wastewater by calcined alkaline residue: Batch and column studies. *Journal of the Taiwan Institute of Chemical Engineers* **2014**, *45* (4), 1709.
(124) Karageorgiou, K.; Paschalis, M.; Anastassakis, G. N. Removal of phosphate species from solution by adsorption onto calcite used as natural adsorbent. *Journal of Hazardous Materials* **2007**, *139* (3), 447.
(125) Li, R.; Kelly, C.; Keegan, R.; Xiao, L.; Morrison, L.; Zhan, X. Phosphorus removal from wastewater using natural pyrrhotite. *Colloids Surf., A* **2013**, *427*, 13.
(126) Woumfo, E. D.; Siewe, J. M.; Njopwouo, D. A fixed-bed column for phosphate removal from aqueous solutions using an andosol-bagasse mixture. *Journal of environmental management* **2015**, *151*, 450.
(127) Shen, H.; Wang, Z.; Zhou, A.; Chen, J.; Hu, M.; Dong, X.; Xia, Q. Adsorption of phosphate onto amine functionalized nano-sized magnetic polymer adsorbents: mechanism and magnetic effects. *RSC Adv.* **2015**, *5* (28), 22080.
(128) Pradhan, J.; Das, J.; Das, S.; Thakur, R. S. Adsorption of Phosphate from Aqueous Solution Using Activated Red Mud. *J. Colloid Interface Sci.* **1998**, *204* (1), 169.
(129) Yang, S.; Zhao, Y.; Chen, R.; Feng, C.; Zhang, Z.; Lei, Z.; Yang, Y. A novel tablet porous material developed as adsorbent for phosphate removal and recycling. *J. Colloid Interface Sci.* **2013**, *396*, 197.
(130) Yuan, X.; Xia, W.; An, J.; Yin, J.; Zhou, X.; Yang, W. Kinetic and Thermodynamic Studies on the Phosphate Adsorption Removal by Dolomite Mineral. *J. Chem.* **2015**, *2015*, 1.
(131) Eljamal, O.; Okawauchi, J.; Hiramatsu, K.; Harada, M. Phosphorus sorption from aqueous solution using natural materials. *Environ. Earth Sci.* **2013**, *68* (3), 859.
(132) Blaney, L. M.; Cinar, S.; SenGupta, A. K. Hybrid anion exchanger for trace phosphate removal from water and wastewater. *Water Res.* **2007**, *41* (7), 1603.
(133) Kim, Y.-S.; Lee, Y.-H.; An, B.; Choi, S.-A.; Park, J.-H.; Jurng, J.-S.; Lee, S.-H.; Choi, J.-W. Simultaneous Removal of Phosphate and Nitrate in Wastewater Using High-Capacity Anion-Exchange Resin. *Water Air Soil Poll.* **2012**, *223* (9), 5959.
(134) Pan, B.; Wu, J.; Pan, B.; Lv, L.; Zhang, W.; Xiao, L.; Wang, X.; Tao, X.; Zheng, S. Development of polymer-based nanosized hydrated ferric oxides (HFOs) for enhanced phosphate removal from waste effluents. *Water Res.* **2009**, *43* (17), 4421.
(135) Koilraj, P.; Kannan, S. Phosphate uptake behavior of ZnAlZr ternary layered double hydroxides through surface precipitation. *J. Colloid Interface Sci.* **2010**, *341* (2), 289.
(136) Lisa, A.; Paras, T. In *Natural Attenuation of Trace Element Availability in Soils*; CRC Press, 2006, DOI: 10.1201/9781420042832.ch4.
(137) Ghaneian, M. T.; Ghanizadeh, G.; Alizadeh, M. T. H.; Ehrampoush, M. H.; Said, F. M. Equilibrium and kinetics of phosphorous adsorption onto bone charcoal from aqueous solution. *Environmental Technology* **2014**, *35* (7), 882.
(138) Fang, L.; Huang, L.; Holm, P. E.; Yang, X.; Hansen, H. C. B.; Wang, D. Facile upscaled synthesis of layered iron oxide nanosheets and their application in phosphate removal. *Journal of Materials Chemistry A* **2015**, *3* (14), 7505.
(139) Zheng, Y.; Wan, Y.; Zhang, Y.; Huang, J.; Yang, Y.; Tsang, D. C.; Wang, H.; Chen, H.; Gao, B. Recovery of phosphorus from wastewater: A review based on current phosphorous removal technologies. *Critical reviews in environmental science and technology* **2023**, *53* (11), 1148.
(140) Drenkova-Tuhtan, A.; Schneider, M.; Mandel, K.; Meyer, C.; Gellermann, C.; Sextl, G.; Steinmetz, H. Influence of cation building blocks of metal hydroxide precipitates on their adsorption and desorption capacity for phosphate in wastewater—A screening study. *Colloids Surf., A* **2016**, *488*, 145.
(141) Xiong, W.; Tong, J.; Yang, Z.; Zeng, G.; Zhou, Y.; Wang, D.; Song, P.; Xu, R.; Zhang, C.; Cheng, M. Adsorption of phosphate from aqueous solution using iron-zirconium modified activated carbon nanofiber: performance and mechanism. *J. Colloid Interface Sci.* **2017**, *493*, 17.
(142) Drenkova-Tuhtan, A.; Schneider, M.; Franzreb, M.; Meyer, C.; Gellermann, C.; Sextl, G.; Mandel, K.; Steinmetz, H. Pilot-scale removal and recovery of dissolved phosphate from secondary wastewater effluents with reusable ZnFeZr adsorbent@ Fe3O4/SiO2 particles with magnetic harvesting. *Water Res.* **2017**, *109*, 77.
(143) Naseef, E. Removal of Phosphates from Industrial Waste Water by Chemical Precipitation. *Engineering Science and Technology: An International Journal* **2012**, *2* (3), 409.
(144) Park, T.; Ampunan, V.; Lee, S.; Chung, E. Chemical behavior of different species of phosphorus in coagulation. *Chemosphere* **2016**, *144*, 2264.
(145) Mehta, C. M.; Khunjar, W. O.; Nguyen, V.; Tait, S.; Batstone, D. J. Technologies to Recover Nutrients from Waste Streams: A Critical

Review. *Critical Reviews in Environmental Science and Technology* **2015**, *45* (4), 385.
(146) Zelmanov, G.; Semiat, R. The influence of competitive inorganic ions on phosphate removal from water by adsorption on iron (Fe+3) oxide/hydroxide nanoparticles-based agglomerates. *J. Water Process. Eng.* **2015**, *5*, 143.
(147) Doyle, J. D.; Parsons, S. A. Struvite formation, control and recovery. *Water Res.* **2002**, *36* (16), 3925.
(148) Huang, H.; Xiao, D.; Liu, J.; Hou, L.; Ding, L. Recovery and removal of nutrients from swine wastewater by using a novel integrated reactor for struvite decomposition and recycling. *Sci. Rep.* **2015**, *5*, 10183.
(149) Wilsenach, J. A.; Schuurbiers, C. A.; van Loosdrecht, M. C. Phosphate and potassium recovery from source separated urine through struvite precipitation. *Water Res.* **2007**, *41* (2), 458.
(150) Zhang, T.; Bowers, K. E.; Harrison, J. H.; Chen, S. Releasing Phosphorus from Calcium for Struvite Fertilizer Production from Anaerobically Digested Dairy Effluent. *Water Environment Research* **2010**, *82* (1), 34.
(151) Quintana, M.; Colmenarejo, M. F.; Barrera, J.; Sánchez, E.; Garcia, G.; Travieso, L.; Borja, R. Removal of phosphorus through struvite precipitation using a by-product of magnesium oxide production (BMP): Effect of the mode of BMP preparation. *Chemical Engineering Journal* **2008**, *136* (2−3), 204.
(152) Pastor, L.; Mangin, D.; Barat, R.; Seco, A. A pilot-scale study of struvite precipitation in a stirred tank reactor: conditions influencing the process. *Bioresource technology* **2008**, *99* (14), 6285.
(153) Le Corre, K. S.; Valsami-Jones, E.; Hobbs, P.; Parsons, S. A. Phosphorus Recovery from Wastewater by Struvite Crystallization: A Review. *Critical Reviews in Environmental Science and Technology* **2009**, *39* (6), 433.
(154) Münch, E. V.; Barr, K. Controlled struvite crystallisation for removing phosphorus from anaerobic digester sidestreams. *Water Res.* **2001**, *35* (1), 151.
(155) Kumar, R.; Pal, P. Assessing the feasibility of N and P recovery by struvite precipitation from nutrient-rich wastewater: a review. *Environmental Science and Pollution Research* **2015**, *22* (22), 17453.
(156) Mehta, C. M.; Batstone, D. J. Nucleation and growth kinetics of struvite crystallization. *Water Res.* **2013**, *47* (8), 2890.
(157) Acelas, N. Y.; Flórez, E.; López, D. Phosphorus recovery through struvite precipitation from wastewater: effect of the competitive ions. *Desalination and Water Treatment* **2015**, *54* (9), 2468.
(158) Jaffer, Y.; Clark, T. A.; Pearce, P.; Parsons, S. A. Potential phosphorus recovery by struvite formation. *Water Res.* **2002**, *36* (7), 1834.
(159) Hutnik, N.; Kozik, A.; Mazienczuk, A.; Piotrowski, K.; Wierzbowska, B.; Matynia, A. Phosphates (V) recovery from phosphorus mineral fertilizers industry wastewater by continuous struvite reaction crystallization process. *Water Res.* **2013**, *47* (11), 3635.
(160) Ronteltap, M.; Maurer, M.; Hausherr, R.; Gujer, W. Struvite precipitation from urine - Influencing factors on particle size. *Water Res.* **2010**, *44* (6), 2038.
(161) Marti, N.; Bouzas, A.; Seco, A.; Ferrer, J. Struvite precipitation assessment in anaerobic digestion processes. *Chemical Engineering Journal* **2008**, *141* (1−3), 67.
(162) Hao, X. D.; Wang, C. C.; Lan, L.; van Loosdrecht, M. C. M. Struvite formation, analytical methods and effects of pH and Ca2+. *Water Sci. Technol.* **2009**, *59* (6), 1077.
(163) Le Corre, K. S.; Valsami-Jones, E.; Hobbs, P.; Jefferson, B.; Parsons, S. A. Agglomeration of struvite crystals. *Water Res.* **2007**, *41* (2), 419.
(164) Jones, A. G. Design of crystallization process systems. In *Crystallization Process Systems*; Butterworth-Heinemann: Oxford, 2002, 261−298, DOI: 10.1016/B978-075065520-0/50010-9.
(165) Bhuiyan, M. I. H.; Mavinic, D. S.; Koch, F. A. Thermal decomposition of struvite and its phase transition. *Chemosphere* **2008**, *70* (8), 1347.
(166) Frost, R. L.; Weier, M. L.; Erickson, K. L. Thermal decomposition of struvite. *J. Therm. Anal. Calorim.* **2004**, *76* (3), 1025.
(167) Antonini, S.; Arias, M. A.; Eichert, T.; Clemens, J. Greenhouse evaluation and environmental impact assessment of different urine-derived struvite fertilizers as phosphorus sources for plants. *Chemosphere* **2012**, *89* (10), 1202.
(168) O'Neal, J. A.; Boyer, T. H. Phosphorus recovery from urine and anaerobic digester filtrate: comparison of adsorption-precipitation with direct precipitation. *Environmental Science: Water Research & Technology* **2015**, *1* (4), 481.
(169) Ganrot, Z.; Dave, G.; Nilsson, E. Recovery of N and P from human urine by freezing, struvite precipitation and adsorption to zeolite and active carbon. *Bioresource technology* **2007**, *98* (16), 3112.
(170) Morales, N.; Boehler, M.; Buettner, S.; Liebi, C.; Siegrist, H. Recovery of N and P from Urine by Struvite Precipitation Followed by Combined Stripping with Digester Sludge Liquid at Full Scale. *Water* **2013**, *5* (3), 1262.
(171) Etter, B.; Tilley, E.; Khadka, R.; Udert, K. M. Low-cost struvite production using source-separated urine in Nepal. *Water Res.* **2011**, *45* (2), 852.
(172) Latifian, M.; Liu, J.; Mattiasson, B. Struvite-based fertilizer and its physical and chemical properties. *Environmental Technology* **2012**, *33* (24), 2691.
(173) Parsons, S. A.; Smith, J. A. Phosphorus removal and recovery from municipal wastewaters. *Elements* **2008**, *4* (2), 109.
(174) Ryu, H.-D.; Lim, C.-S.; Kim, Y.-K.; Kim, K.-Y.; Lee, S.-I. Recovery of Struvite Obtained from Semiconductor Wastewater and Reuse as a Slow-Release Fertilizer. *Environmental Engineering Science* **2012**, *29* (6), 540.
(175) Spangberg, J.; Tidaker, P.; Jonsson, H. Environmental impact of recycling nutrients in human excreta to agriculture compared with enhanced wastewater treatment. *Sci. Total Environ.* **2014**, *493*, 209.
(176) Bonvin, C.; Etter, B.; Udert, K. M.; Frossard, E.; Nanzer, S.; Tamburini, F.; Oberson, A. Plant uptake of phosphorus and nitrogen recycled from synthetic source-separated urine. *Ambio* **2015**, *44*, 217.
(177) Gaterell, M. R.; Gay, R.; Wilson, R.; Gochin, R. J.; Lester, J. N. An Economic and Environmental Evaluation of the Opportunities for Substituting Phosphorus Recovered from Wastewater Treatment Works in Existing UK Fertiliser Markets. *Environmental Technology* **2000**, *21* (9), 1067.
(178) Winker, M.; Vinneras, B.; Muskolus, A.; Arnold, U.; Clemens, J. Fertiliser products from new sanitation systems: their potential values and risks. *Bioresource technology* **2009**, *100* (18), 4090.
(179) Daneshgar, S.; Vanrolleghem, P. A.; Vaneeckhaute, C.; Buttafava, A.; Capodaglio, A. G. Optimization of P compounds recovery from aerobic sludge by chemical modeling and response surface methodology combination. *Science of the total environment* **2019**, *668*, 668.
(180) Yee, R. A.; Leifels, M.; Scott, C.; Ashbolt, N. J.; Liu, Y. Evaluating microbial and chemical hazards in commercial struvite recovered from wastewater. *Environ. Sci. Technol.* **2019**, *53* (9), 5378.
(181) Egle, L.; Rechberger, H.; Krampe, J.; Zessner, M. Phosphorus recovery from municipal wastewater: An integrated comparative technological, environmental and economic assessment of P recovery technologies. *Science of the total environment* **2016**, *571*, 522.
(182) Nakarmi, A.; Kanel, S.; Nadagouda, M. N.; Viswanathan, T. In *Green functionalized nanomaterials for environmental applications*; Elsevier, 2022.
(183) Daneshgar, S.; Buttafava, A.; Callegari, A.; Capodaglio, A. G. Economic and energetic assessment of different phosphorus recovery options from aerobic sludge. *Journal of Cleaner Production* **2019**, *223*, 729.